ABSTRACT

THIRUNAVUKKARASU, SENGANAL. Absorbing Boundary Conditions for Molecular Dynamics. (Under the direction of Professor Murthy N. Guddati).

With the goal of minimizing the domain size for Molecular dynamics (MD) simulations, we develop a new class of absorbing boundary conditions (MD-ABC's) that can mimic the phonon absorption of an unbounded exterior. The proposed MD-ABC's are extensions of perfectly matched discrete layers (PMDL), originally developed as an absorbing boundary condition for continuous wave propagation problems. Called MD-PMDL, this extension carefully targets the absorption of phonons, the high frequency waves, whose propagation properties are completely different from continuous waves.

This thesis presents the derivation of MD-PMDL for general lattice systems, followed by explicit application to one-dimensional and two-dimensional square lattice systems.The accuracy of MD-PMDL for phonon absorption is proven by analyzing reflection coefficients, and demonstrated through numerical experiments. Unlike existing ABC's that are effective for high frequency phonon absorption, MD-PMDL is local in both space and time and is thus more efficient. Based on their favorable properties, it is concluded that MD-PMDL could provide a more effective alternative to existing MD-ABC's.

Absorbing Boundary Conditions for Molecular Dynamics

by
Senganal Thirunavukkarasu

A thesis submitted to the Graduate Faculty of
North Carolina State University
in partial fullfillment of the
requirements for the Degree of
Master of Science

Civil Engineering

Raleigh, North Carolina

2008

APPROVED BY:

Dr. P. A. Gremaud	Dr. M. S. Rahman

Dr. M. N. Guddati
Chair of Advisory Committee

BIOGRAPHY

Senganal Thirunavukkarasu was born in India on July 22, 1981, the son of Govindasamy Thirunavukkarasu and Thirunavukkarasu Shanthi. In July 2003, he was awarded his B. Tech. degree in Civil Engineering from the Indian Institute of Technology Madras, India. He then worked as a Software Engineer in the IT industry for a period of 3 years. In August 2006, he entered the Graduate School at North Carolina State University.

ACKNOWLEDGMENTS

The author would like to express his immense gratitude and deep admiration for the supervisor of this thesis Dr.M.N.Guddati who has granted him the opportunity to learn so much through the accomplishment of the present work. The author would also like to thank Dr.M.S.Rahman and Dr.P.A.Gremaud for their time serving as the members of the advisory committee. Their comments and suggestions are gratefully acknowledged.

TABLE OF CONTENTS

LIST OF FIGURES

Chapter 1

Introduction

Molecular Dynamics (MD) is a widely used method to study physical phenomenon at the atomic scale. It offers valuable insights into the behavior of certain macroscopic processes, like fracture, that are fundamentally triggered at the atomistic scale. One of the major problems in using MD simulation to study such processes is the computational expense involved in simulating a large system. To make the simulation tractable, the MD domain is usually truncated with simple (Dirichlet/Neumann/Periodic) boundary conditions applied at the boundary. However, a simple boundary condition would result in significant energy being artificially reflected back into the region of interest and can completely distort the physical phenomenon being studied. To minimize this error, the simulation domain is taken to be much larger than the region of interest which significantly increases the computational expense of the simulation. This can be avoided by using a more appropriate boundary condition that mimics the effect of the exterior at the truncated boundary. Applying such a boundary condition would necessitate a much smaller computational domain, thus resulting in significant savings in computational expense.

The problem discussed above is similar to the problem of suppressing artificial reflections at a truncated boundary of an infinite domain in continuum wave propagation. This problem has been studied extensively and there exist boundary conditions called Absorbing Boundary Conditions (ABC's) that are quite effective in absorbing the incoming energy thus mimicking the exterior[1]. It seems natural to try and extend these boundary conditions to the discrete domain encountered in MD. However, the spectrum of waves (phonons) generated in the MD domain spreads over all frequencies which for continuum

wave propagation is not the case where the frequencies are low. Thus, ABC's developed for continuous wave propagation would not be able to handle the high frequency phonons generated in the MD domain. Instead, ABC's are to be derived explicitly for discrete domains. Many ABC's are developed for this purpose and the following is a summary.

Exact boundary conditions based on the Green's function of the exterior

In this approach, the exact boundary condition is found as the response function at the interface. The main problem is that these boundary conditions are non-local in space and time. In [2], Cai et al. propose methods to numerically obtain these boundary conditions for square lattice structures by computing response functions for the boundary. Liu and co-workers have extended the idea of Green's function for more general crystals [3, 4]. Though exact boundary conditions can be derived, they are difficult to implement as they are non-local in both space and time. Since the response functions decay rather slowly, this coupling in time makes the BC's computationally very expensive.

Perfectly Matched Layers (PML type methods)

The PML method is a continuum ABC and is based on the idea that propagating waves are damped in complex space [5, 6]. The method involves appending to the computational domain, a border region that is stretched into complex space. This complex border region essentially acts like a lossy material and dissipates any incoming energy thereby reducing the reflection into the domain. While continuous PML may have the disadvantage of being less efficient than rational ABC's [7], it can be considered highly successful, owing to its flexibility. An extension of PML to discrete problems is explored by S. Li and co-workers [8, 9]. While the extension is valid for low frequency waves, it can be shown that it is not accurate for high frequency phonons that are central to discrete ABC's.

Variational boundary conditions (VBC's)

E and co-workers tackle the problem from a optimization view point by using variational principles to minimize the total phonon reflection [10, 11]. The main advantage of VBC is its generality; theoretically, the procedure is applicable to complex lattice systems. While VBC's appear to perform better than the Green's function based methods and PML

based methods, they still involve expensive convolution operations and are computationally expensive. Also, their long-term stability properties are not clear. Though appropriate stabilization can be performed through explicit constraints, such constraints appear to degrade the performance of the method. Other minor shortcomings of the method are the lack of transparency in the approximation properties of the method and ease of extension to corners.

Proposed Absorbing Boundary Conditions

In this thesis, we present a new direction for developing ABC's for Molecular dynamics. The basic ideas stem from earlier research linking PML with local absorbing boundary conditions [12] to create a class of boundary conditions called Perfectly Matched Discrete Layers(PMDL)[13]. PMDL is essentially PML discretized using linear finite elements with mid-point integration. It was shown that the integration error exactly cancels the discretization error, thus resulting in perfect matching even after the discretization of the exterior. Furthermore, it was shown that PMDL is equivalent to rational-approximation based ABC's and thus inherits their efficiency while retaining the flexibility of PML. The main limitation, however, is that PMDL is perfectly matched with the continuous interior, but not with the discrete interior. Thus PMDL, like other ABC's for wave equation, works well for low frequency limits, but fails in absorbing high frequency phonons.

The main contribution of this thesis is to show that PMDL can be utilized to absorb even high frequency phonons. The key idea is that PMDL can be viewed as a discrete lattice with non-uniform spacing that has the special property of the characteristic impedance being independent of the atomic spacing. It is then shown that, for a particular choice of parameters, the PMDL lattice can be made algebraically identical to a general periodic harmonic lattice. Since the PMDL lattice has the additional property of being perfectly matched irrespective of the spacing, any phonon reflections that are introduced due to the truncation of the lattice can be damped out using a few exterior atoms with complex atomic spacing. Thus PMDL can be extended in a systematic manner to to yield highly accurate boundary conditions for discrete systems, called MD-PMDL, that are similar in form to PMDL and requires slightly more computational effort. Compared to existing methods for discrete systems, the proposed method shows promise in providing a more efficient and systematic boundary condition. It should be noted that while MD-PMDL is similar in

spirit to PML/PMDL boundary conditions, it is not the same as applying PML/PMDL discretization to the continuum limit equation of the original harmonic lattice. We present both analytical and numerical results that demonstrate this crucial difference.

The outline of the rest of the thesis is as follows. The basic problem setup is presented in Chapter 2 with the help of one-dimensional Frenkel-Kontorova model. Since MD-PMDL is closely related to PMDL, a summary of PMDL ABC's is provided in Chapter 3, and the extension to the discrete interior is explained in Chapter 4. The formulation of MD-PMDL including *a-priori* error analysis and a numerical example is presented in Chapter 5. The extension of MD-PMDL to a square lattice along with numerical examples is presented in Chapter 6 and the thesis is concluded with some closing remarks in Chapter 7.

Chapter 2

Problem Setup

We choose the 1-D Frenkel-Kontorova(FK) model to illustrate the ideas in a 1-D setting. A lattice is an infinite chain of atoms with mass m that are spaced apart at a distance h(see Fig(2.1a)). The atoms are labeled with fractional indices, while integer indices are used for the interconnecting cells.

The governing equations for the FK model is given by:

$$\begin{aligned} m\ddot{u}_{j+\frac{1}{2}} &= p\left(u_{j+\frac{3}{2}} - 2u_{j+\frac{1}{2}} + u_{j-\frac{1}{2}}\right) - V'_{ext}(x_{j+\frac{1}{2}}) + f^{ext}_{j+\frac{1}{2}}, \\ x_{j+\frac{1}{2}} &= (j+\frac{1}{2})h + u_{j+\frac{1}{2}} \quad \text{for} \quad j = -\infty \ldots \infty, \end{aligned} \tag{2.1}$$

where u is the displacement field of the atoms, V_{ext} is an external potential field and p describes the strength of nearest-neighbor interaction between the atoms. Let us consider a partition of the 1D infinite lattice into interior and exterior atoms, corresponding to negative and positive indices respectively. This results in the partitioning of the cells into 3 regions (interior, boundary and exterior) as shown in Fig(2.1b). The interior is essentially the region of interest in the MD simulation, while the exterior is to be replaced by an MD-ABC. Specifically, the goal is to devise an MD-ABC at $x_{\frac{1}{2}}$ that mimics the absorption properties of the exterior. It should be emphasized that the dynamics of the exterior is important *only* at the interface as we are interested merely in the propagation of energy from the interior into the exterior.

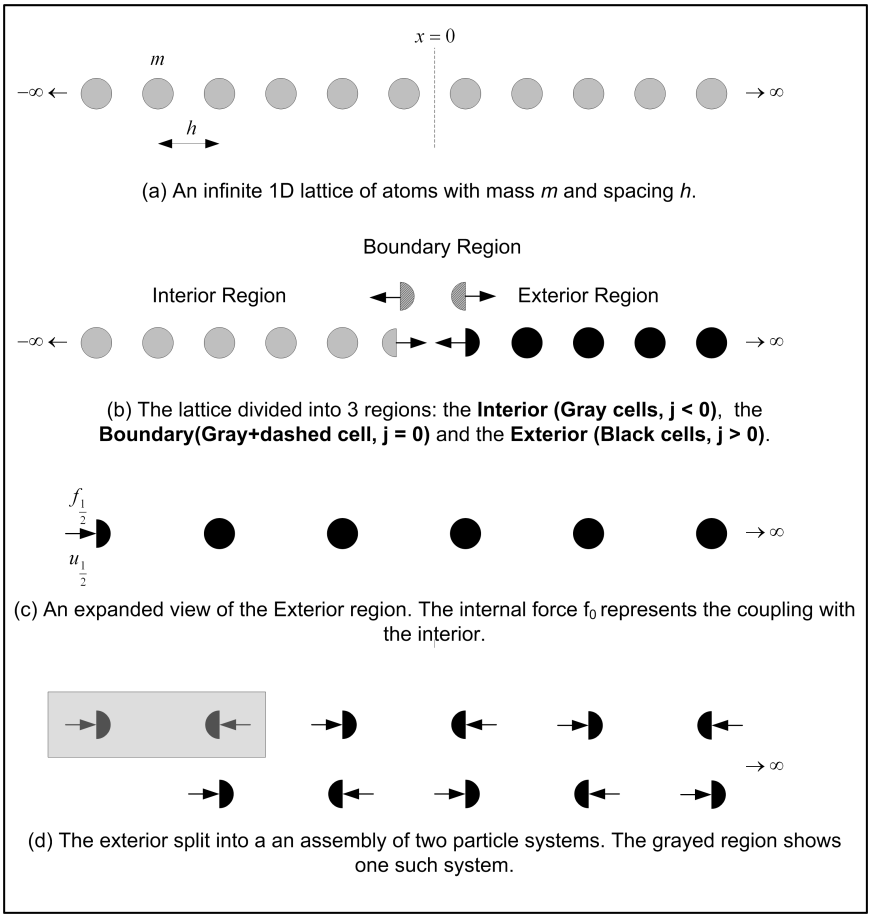

(a) An infinite 1D lattice of atoms with mass *m* and spacing *h*.

(b) The lattice divided into 3 regions: the **Interior (Gray cells, j < 0)**, the **Boundary(Gray+dashed cell, j = 0)** and the **Exterior (Black cells, j > 0)**.

(c) An expanded view of the Exterior region. The internal force f_0 represents the coupling with the interior.

(d) The exterior split into a an assembly of two particle systems. The grayed region shows one such system.

Figure 2.1: Schematic of an infinite 1-D lattice.

2.1 Harmonic Approximation of the Exterior

The potential field is assumed to be a harmonic function in the exterior (this is typical for the development of most MD-ABC's; it appears important to include the entire nonlinear region in the interior). This is a reasonable assumption as the exterior is far away from the region of activity and the displacements of the atoms in the exterior are small. Under this assumption, the force due to the external potential, i.e $V'(x)$, can be approximated by:

$$V'_{ext}\left(x_{j+\frac{1}{2}}\right) = l\, u_{j+\frac{1}{2}}, \tag{2.2}$$

where $l = V''_{ext}(\left(j+\frac{1}{2}\right)h)$ is the force constant and can be found by evaluating the linearized force due the potential about the equilibrium positions. Thus, (2.1) can be written in frequency domain as :

$$-aD^2 u_{j+\frac{1}{2}} - bu_{j+\frac{1}{2}} = f^{ext}_{j+\frac{1}{2}}, \quad j = 0, .., \infty, \tag{2.3}$$

where $a = ph^2$, $b = m\omega^2 - l$ and D^2 is the central difference operator given by:

$$D^2 u_j = \frac{1}{h^2}\left(u_{j+1} - 2u_j + u_{j-1}\right). \tag{2.4}$$

The reduced equation (2.3) is also known as the discrete wave equation and is used to model the transportation of energy in a lattice. The propagation of energy in a lattice is usually modeled as the propagation of discrete waves, called phonons, that are governed by the discrete wave equation. Thus the discrete wave equation (2.3) will be used as the governing equation for the exterior.

2.2 The Assembly Operator

A lattice is a periodic structure with a unit cell being the basis. Thus it is natural to express the lattice as an assembly of unit cells as shown in Fig(1d). To make the subsequent discussions simpler, the finite element assembly operator is used to represent (2.3) in a concise form. The assembly operator and the modified equations are discussed next.

Let the equation for an individual unit cell i be given by:

$$\begin{bmatrix} a_i & -b_i \\ -b_i & a_i \end{bmatrix} \mathbf{u_i} = \mathbf{f_i} \tag{2.5}$$

where $\mathbf{u_i}^t = \begin{bmatrix} u_{i-\frac{1}{2}} & u_{i+\frac{1}{2}} \end{bmatrix}$ are the displacements of the left and right atoms, and $\mathbf{f_i}^t = \begin{bmatrix} f_{i-\frac{1}{2}} & f_{i+\frac{1}{2}} \end{bmatrix}$ are the corresponding forces from the rest of the lattice. The assembly operator, $\mathbb{A}$, is defined as follows:

$$\begin{aligned} \left(\mathop{\mathbb{A}}_{i=-\infty}^{\infty} \begin{bmatrix} a & b \\ c & d \end{bmatrix} \right) &= \begin{bmatrix} \ddots & & & \\ & c & a+d & b \\ & & & \ddots \end{bmatrix} \\ \left(\mathop{\mathbb{A}}_{i=-\infty}^{\infty} \begin{Bmatrix} a \\ b \end{Bmatrix} \right) &= \begin{Bmatrix} \vdots \\ b+a \\ \vdots \end{Bmatrix} \end{aligned} \tag{2.6}$$

where i represents the unit cell index. Using the above definitions, the 1D discrete wave equation can now be written as:

$$\left(\mathop{\mathbb{A}}_{i=-\infty}^{\infty} \begin{bmatrix} a - \frac{b}{2} & -a \\ -a & a - \frac{b}{2} \end{bmatrix} \right) \mathbf{U} = \mathbf{F}. \tag{2.7}$$

The assembly operation can also be defined for the case of a 2D lattice in a similar way. Consider a 2D cell given by:

$$\mathbf{Au} = \mathbf{f} \implies \begin{bmatrix} a_{11} & a_{12} & a_{13} & a_{14} \\ a_{21} & a_{22} & a_{23} & a_{24} \\ a_{31} & a_{32} & a_{33} & a_{34} \\ a_{41} & a_{42} & a_{43} & a_{44} \end{bmatrix} \begin{Bmatrix} u_1 \\ u_2 \\ u_3 \\ u_4 \end{Bmatrix} = \begin{Bmatrix} f_1 \\ f_2 \\ f_3 \\ f_4 \end{Bmatrix}, \tag{2.8}$$

where u_1, u_2, u_3 and u_4 are the displacements at the nodes of the cell. Then the 2D assembly can be written as

$$\left(\mathop{\mathbb{A}}_{\substack{i=-\infty,..,\infty \\ j=-\infty,..,\infty}} \{\mathbf{A}\} \right) \mathbf{U} = \left(\mathop{\mathbb{A}}_{\substack{i=-\infty,..,\infty \\ j=-\infty,..,\infty}} \{\mathbf{f}\} \right) \tag{2.9}$$

where $\underset{\substack{i=-\infty,..,\infty \\ j=-\infty,..,\infty}}{\mathbb{A}} \{\}$ is called the 2D assembly operator and is defined as

$$\underset{\substack{i=-\infty,..,\infty \\ j=-\infty,..,\infty}}{\mathbb{A}} \{\mathbf{A}\} = \begin{bmatrix} & & m_1 & \dots & m_2 & \dots & m_3 & \dots & m_4 & \dots \\ & & \downarrow & & \downarrow & & \downarrow & & \downarrow & \\ m_1 & \rightarrow & .. + a_{11} & & .. + a_{12} & & .. + a_{13} & & .. + a_{14} & \\ \vdots & & & & & & & & & \\ m_2 & \rightarrow & .. + a_{21} & & .. + a_{22} & & .. + a_{23} & & .. + a_{24} & \\ \vdots & & & & & & & & & \\ m_3 & \rightarrow & .. + a_{31} & & .. + a_{32} & & .. + a_{33} & & .. + a_{34} & \\ \vdots & & & & & & & & & \\ m_4 & \rightarrow & .. + a_{41} & & .. + a_{42} & & .. + a_{43} & & .. + a_{44} & \\ \vdots & & & & & & & & & \end{bmatrix}, \tag{2.10}$$

$$\underset{\substack{i=-\infty,..,\infty \\ j=-\infty,..,\infty}}{\mathbb{A}} \{\mathbf{f}\} = \begin{Bmatrix} m_1 & \rightarrow & .. + f_1 \\ \vdots & & \\ m_2 & \rightarrow & .. + f_2 \\ \vdots & & \\ m_3 & \rightarrow & .. + f_3 \\ \vdots & & \\ m_4 & \rightarrow & .. + f_4 \\ \vdots & & \end{Bmatrix}, \tag{2.11}$$

where m_1, m_2, m_3 and m_4 are the indices of the displacements u_1, u_2, u_3 and u_4 in the assembled system $\mathbf{U}$.

2.3 Problem Statement for a 1D Periodic Lattice

To make the subsequent discussions generic to any harmonic and periodic lattice, the governing equations are assumed to be

$$\left(\underset{i=-\infty}{\overset{\infty}{\mathbb{A}}} \begin{bmatrix} p & q \\ r & p \end{bmatrix} \right) \mathbf{U} = \mathbf{F}, \tag{2.12}$$

where p, q and r depend on the specific governing equation.

Let $\mathbf{u_i}$, $\mathbf{f_i}$ be the displacement and force vectors for the interior and $\mathbf{u_e}$, $\mathbf{f_e}$ be displacement and force vectors for the exterior i.e.,

$$\mathbf{u_i} = \begin{Bmatrix} u_{-\infty} \\ \vdots \\ u_{-\frac{1}{2}} \end{Bmatrix}, \ \mathbf{f}_i = \begin{Bmatrix} f_{-\infty} \\ \vdots \\ f_{-\frac{1}{2}} \end{Bmatrix} \quad \text{and} \quad \mathbf{u_e} = \begin{Bmatrix} u_{\frac{1}{2}} \\ \vdots \\ u_{\infty} \end{Bmatrix}, \ \mathbf{f_e} = \begin{Bmatrix} f_{\frac{1}{2}} \\ \vdots \\ f_{\infty} \end{Bmatrix}. \tag{2.13}$$

The discrete system (2.12) can now be written as,

$$\begin{bmatrix} \mathbf{A_{ii}} & \mathbf{0} \\ \mathbf{0} & \mathbf{A_{ee}} \end{bmatrix} \begin{Bmatrix} \mathbf{u_i} \\ \mathbf{u_e} \end{Bmatrix} = \begin{Bmatrix} \bar{\mathbf{f}}_\mathbf{i} \\ \bar{\mathbf{f}}_\mathbf{e} \end{Bmatrix}, \tag{2.14}$$

where $\mathbf{A_{ii}}$ and $\mathbf{A_{ee}}$ are given by:

$$\begin{aligned} \mathbf{A_{ii}} &= \hat{\mathbf{P}} + \left(\mathop{\mathbb{A}}_{i=-\infty}^{-1} \begin{bmatrix} p & q \\ r & p \end{bmatrix} \right), \quad \hat{\mathbf{P}} = \begin{bmatrix} \ddots & & \vdots \\ & 0 & 0 \\ \dots & 0 & p \end{bmatrix}, \\ \mathbf{A_{ee}} &= \bar{\mathbf{P}} + \left(\mathop{\mathbb{A}}_{i=1}^{\infty} \begin{bmatrix} p & q \\ r & p \end{bmatrix} \right), \quad \bar{\mathbf{P}} = \begin{bmatrix} p & 0 & \dots \\ 0 & 0 & \\ \vdots & & \ddots \end{bmatrix}, \end{aligned} \tag{2.15}$$

and $\bar{\mathbf{f}}_\mathbf{i}$, $\bar{\mathbf{f}}_\mathbf{e}$ are given by:

$$\bar{\mathbf{f}}_\mathbf{i} = \mathbf{f_i} - \begin{Bmatrix} 0 \\ \vdots \\ q u_{\frac{1}{2}} \end{Bmatrix}, \quad \text{and} \quad \bar{\mathbf{f}}_\mathbf{e} = \mathbf{f_e} - \begin{Bmatrix} r u_{-\frac{1}{2}} \\ 0 \\ \vdots \end{Bmatrix}. \tag{2.16}$$

Note that in (2.16), the interior is coupled to the exterior through the displacement at $i = \frac{1}{2}$ and thus to solve the interior we only need the displacement at $i = \frac{1}{2}$. Also, note that $\bar{\mathbf{f}}_\mathbf{e}$ is zero except at $i = \frac{1}{2}$. Thus, $u_{\frac{3}{2}, \frac{5}{2}, .. \infty}$ can be eliminated and the effect of the exterior can be written solely in terms of $u_{\frac{1}{2}}$. This is essentially the Dirichlet-to-Neumann relation for the exterior and can be written as

$$K u_{\frac{1}{2}} = f_{\frac{1}{2}}, \tag{2.17}$$

where K is the Dirichlet-to-Neumann(DtN) map for the exterior. K is also commonly referred to as the discrete half-space stiffness and both terms will be used interchangeably in subsequent discussions.

The goal of the MD-ABC can be restated as approximating the DtN map, or the discrete half-space stiffness, of the exterior. This is analogous to the problem of approximating the DtN map of a continuous half-space in wave propagation. This problem has been studied extensively and there exist mature continuous methods that approximate the DtN map in an accurate and efficient manner. We choose a particular class of ABC's called Perfectly Matched Discrete Layers (PMDL) for its generality and flexibility [12, 13]. The PMDL boundary conditions are summarized in the next chapter.

Chapter 3

A Summary of Perfectly Matched Discrete Layer (PMDL)

3.1 PMDL for the Scalar Wave Equation

PMDL is a class of ABC that approximates the stiffness of a continuous half-space [13]. Though PMDL is applicable to any second order system [14], for the sake of simplicity the central ideas are summarized using a one dimensional scalar wave equation. Consider a right half-space with left boundary at $x = 0$ as shown in Fig(3.1a). Let the governing equation be given by

$$-\frac{\partial^2 u}{\partial x^2} - \Lambda u = 0, \tag{3.1}$$

where Λ is a differential operator. Equation (3.1) can be written as

$$-\left(\frac{\partial}{\partial} - \mathrm{i}\sqrt{\Lambda}\right)\left(\frac{\partial}{\partial} + \mathrm{i}\sqrt{\Lambda}\right) u = 0, \tag{3.2}$$

where first factor represents forward propagating waves while the second factor represents backward propagating waves. When the excitation is limited to the boundary, x=0, waves propagate only in the positive x direction (since the half-space does not reflect any waves). This translates into a relation

$$\frac{\partial u}{\partial x} - ik_x u = 0, \quad k_x = +\sqrt{\Lambda}, \tag{3.3}$$

where k_x is the wave number. Equation (3.3) can be viewed as a relationship between Dirichlet and Neumann data at the boundary x=0. This relation is deceptively simple;

note that k_x is a square-root of the differential operator Λ. Due to the irrational nature of the square-root operator, k_x is a pseudo differential operator involving expensive convolution operations. Traditionally the computational expense is reduced by approximating the square-root operator with a rational function, thus leading to a differential form of (3.3).

The above procedure of factorization and rational approximation is not possible for all wave equations. PMDL takes a different route and completely circumvents the need for explicit factorization or rational approximation. PMDL derivation instead involves a multi-step procedure based on complex coordinate stretching and special finite-element discretization of the half-space, which eventually results in a robust approximation of the half-space impedance, and thus in an effective one-way wave equation. The steps of the derivation are given below.

Step 1

Split the half-space $(0, \infty)$ into a finite element $(0, L)$ and another half-space (L, ∞) , with the finite element discretized using linear shape functions as shown in Fig(3.1b). The stiffness matrix of the finite element layer can be easily derived as,

$$K_{fe} = \begin{bmatrix} \tilde{a} & \tilde{b} \\ \tilde{b} & \tilde{a} \end{bmatrix}, \quad \text{where} \quad \begin{cases} \tilde{a} = \frac{1}{L} - k_x^2 \frac{L}{2}, \\ \tilde{b} = -\frac{1}{L}. \end{cases} \tag{3.4}$$

Considering that there is no excitation at the interior node at $x = L$, the assembled finite-element equations take the form,

$$\begin{bmatrix} \tilde{a} & \tilde{b} \\ \tilde{b} & \tilde{a} + K_{exact} \end{bmatrix} \begin{Bmatrix} u_0 \\ u_1 \end{Bmatrix} = \begin{Bmatrix} f_0 \\ 0 \end{Bmatrix}, \tag{3.5}$$

where K_{exact} is the stiffness of the right half-space, F_0 is the Neumann data at $x = 0$, u_0 and u_1 are the displacements at $x = 0$ and $x = L$. Eliminating u_1 from (3.5), results in:

$$F_0 = \left(\tilde{a} - \frac{\tilde{b}^2}{\tilde{a} + K_{exact}} \right) u_0. \tag{3.6}$$

The above equation is a relationship between the Dirichlet and Neumann data of the discretized half-space. The term in the parentheses is effectively the stiffness of the composite half-space. It can be clearly seen that the above relationship is approximate in that, if exact

half-space stiffness is substituted for the right half-space, i.e. $K_{exact} = -ik_x$, the resulting composite half-space stiffness is not recovered (this can be verified easily with the help of (3.4)).

Step 2

This step is the key to the development of PMDL and involves the elimination of the finite-element discretization error (with respect to the half-space stiffness at $x = 0$). This is achieved by simply using midpoint integration to approximately evaluate the finite element stiffness matrix, i.e.,

$$K_{fe-layer}^{mid-pt} = \begin{bmatrix} a & b \\ b & a \end{bmatrix}, \quad \text{where} \quad \begin{cases} a = \frac{1}{L} - k_x^2 \frac{L}{4}, \\ b = -\frac{1}{L} - k_x^2 \frac{L}{4}. \end{cases} \tag{3.7}$$

When the above approximation is used, we get the following relationship between the stiffnesses of the composite half-space and the right half-space:

$$K_{composite} = \left(a - \frac{b^2}{a + K_{exact}} \right). \tag{3.8}$$

It is easy to verify that, when the exact stiffness, $-ik_x$, is substituted for K_{exact} , we obtain $K_{composite} = -ik_x$, which is also exact (this can be clearly seen by noting that $a^2 - b^2 = K_{exact}^2$). Note that the relationship is exact irrespective of the element length L; it can be arbitrarily large and even complex.

Step 3

The above splitting is recursively applied to discretize the original half-space into infinite number of finite element layers, i.e $\bigcup_{j=1}^{\infty} (x_{j-1}, x_j)$, without introducing any discretization errors. This is equivalent to saying that the assembly,

$$\left(\mathop{\mathbb{A}}_{j=1}^{\infty} \left\{ \frac{1}{L_j} \begin{bmatrix} 1 & -1 \\ -1 & 1 \end{bmatrix} - \frac{k_x^2 L_j}{4} \begin{bmatrix} 1 & 1 \\ 1 & 1 \end{bmatrix} \right\} \right), \quad \text{where} \quad L_j = x_j - x_{j-1}, \tag{3.9}$$

is an exact representation of the the half-space stiffness at $x = 0$.

Step 4

For reasons of computability, the number of layers is limited to n, with Dirichlet boundary condition applied at $x = x_n$ as shown in Fig(3.1d). However, imposing a Dirichlet boundary condition results in complete reflection of any incoming wave and hence these elements would fail to act as an ABC. This is handled by using the idea that propagating waves are damped out by complex media. By choosing the lengths of the finite element to be complex (see Fig.3.1e) the incoming energy into the PMDL elements can be damped out and thus the reflections can be reduced significantly.

3.2 PMDL for a General Second Order Vector Equation

While the arguments in the previous section are explained in the context of scalar wave equation, they are also valid for any second order vector equation [14]. Specifically, it is shown in [14] that the half-space for a system governed by a second order vector equation of the form,

$$-\mathbf{A}\frac{\partial^2 \mathbf{u}}{\partial x^2} + \mathbf{B}\frac{\partial \mathbf{u}}{\partial x} + \mathbf{C}\mathbf{u} = 0, \tag{3.10}$$

can be replaced by the infinite assembly:

$$\underset{i=1}{\overset{\infty}{\mathbb{A}}} \left\{ \frac{1}{L_i} \begin{bmatrix} \mathbf{A} & -\mathbf{A} \\ -\mathbf{A} & \mathbf{A} \end{bmatrix} + \frac{1}{2} \begin{bmatrix} -\mathbf{B} & \mathbf{B} \\ -\mathbf{B} & \mathbf{B} \end{bmatrix} + \frac{1}{4} L_i \begin{bmatrix} \mathbf{C} & \mathbf{C} \\ \mathbf{C} & \mathbf{C} \end{bmatrix} \right\} \mathbf{U_e} = \mathbf{F_e}, \tag{3.11}$$

that preserves the DtN map of the original system at the interface $x = 0$. The assembly operator in (3.11) can be rewritten as an assembly of Kronecker products, i.e.

$$\underset{i=1}{\overset{\infty}{\mathbb{A}}} \left\{ \frac{1}{L_i} \begin{bmatrix} 1 & -1 \\ -1 & 1 \end{bmatrix} \otimes \mathbf{A} + \begin{bmatrix} -1 & 1 \\ -1 & 1 \end{bmatrix} \otimes \frac{1}{2}\mathbf{B} + L_i \begin{bmatrix} 1 & 1 \\ 1 & 1 \end{bmatrix} \otimes \frac{1}{4}\mathbf{C} \right\}. \tag{3.12}$$

If we define basis matrices as,

$$\mathbf{A_{-1}} = \begin{bmatrix} 1 & -1 \\ -1 & 1 \end{bmatrix}, \quad \mathbf{A_0} = \begin{bmatrix} -1 & 1 \\ -1 & 1 \end{bmatrix} \quad \text{and} \quad \mathbf{A_1} = \begin{bmatrix} 1 & 1 \\ 1 & 1 \end{bmatrix}, \tag{3.13}$$

and coefficient matrices as,

$$\mathbf{C_{-1}} = \mathbf{A}, \quad \mathbf{C_0} = \frac{\mathbf{B}}{\mathbf{2}} \quad \text{and} \quad \mathbf{C_1} = \frac{\mathbf{C}}{\mathbf{4}}, \tag{3.14}$$

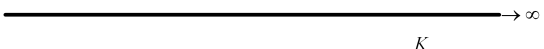

(a) A continuous half-space

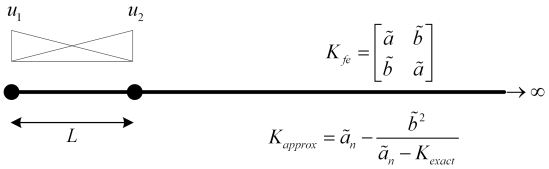

(b) A half-space replaced with a linear finite element + half-space. The stiffness of the assembly is not equal to the exact half-space stiffness.

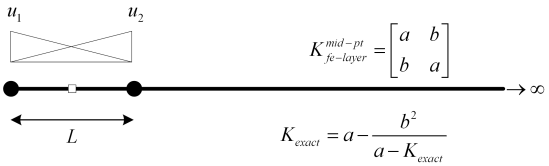

(c) The finite element stiffness is calculated using mid-point integration. The stiffness of the assembly is equal to the exact half-space stiffness irrespective of the element length L.

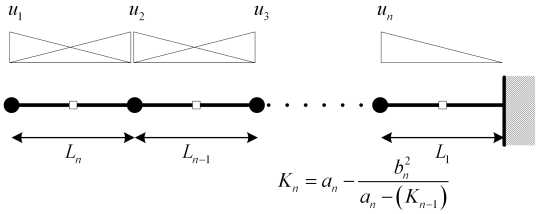

(d) Step(c) is performed recursively to replace half-space with mid-point integrated finite elements. The assembly is truncated after n elements to obtain a finite system. The truncation using a fixed boundary would result in reflections and thus the system fails to act as a half-space.

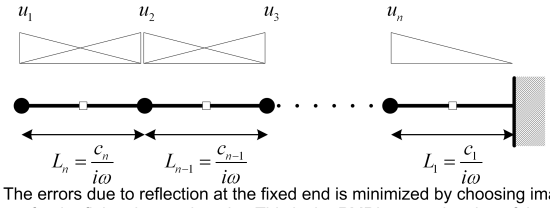

(e) The errors due to reflection at the fixed end is minimized by choosing imaginary values for the finite element lengths. This is the PMDL approximation of the original half-space in (a).

Figure 3.1: Steps in the formulation of PMDL

then (3.12) can be expressed concisely as

$$\left(\mathop{\mathbb{A}}_{i=1}^{\infty} \left\{ \sum_{f\in\{-1,0,1\}} L_i^f \mathbf{A}_f \otimes \mathbf{C}_f \right\} \right) \mathbf{U_e} = \mathbf{F_e}. \tag{3.15}$$

Chapter 4

MD-PMDL: An Extension of PMDL for Molecular Dynamics

In section (2.3), it was shown that the exterior of a harmonic lattice can be expressed as

$$\left(\bar{\mathbf{P}} + \mathop{\mathbb{A}}_{i=1}^{\infty}\left\{\begin{bmatrix} p & q \\ r & p \end{bmatrix}\right\}\right)\mathbf{U_e} = \mathbf{F_e}, \tag{4.1}$$

where $\bar{\mathbf{P}}$ is defined in (2.15). In fact, for the more generic vector system, the exterior can be expressed as

$$\left(\bar{\mathbf{P}} + \mathop{\mathbb{A}}_{i=1}^{\infty}\left\{\begin{bmatrix} \mathbf{P} & \mathbf{Q} \\ \mathbf{R} & \mathbf{P} \end{bmatrix}\right\}\right)\mathbf{U_e} = \mathbf{F_e}, \tag{4.2}$$

where $\mathbf{P}, \mathbf{Q}$ and $\mathbf{R}$ are stiffness matrices that describe the interaction between the unit cells. Note that (4.2) can be rewritten as

$$\left(\bar{\mathbf{P}} + \mathop{\mathbb{A}}_{i=1}^{\infty}\left\{\begin{bmatrix} 1 & -1 \\ -1 & 1 \end{bmatrix} \otimes \mathbf{P}_{-1} + \begin{bmatrix} -1 & 1 \\ -1 & 1 \end{bmatrix} \otimes \mathbf{P}_0 + \begin{bmatrix} 1 & 1 \\ 1 & 1 \end{bmatrix} \otimes \mathbf{P}_1\right\}\right)\mathbf{U_e} = \mathbf{F_e} \tag{4.3}$$

where

$$\mathbf{P}_{-1} = \frac{\mathbf{P}}{2} - \frac{\mathbf{Q}+\mathbf{R}}{4}, \quad \mathbf{P}_0 = \frac{\mathbf{Q}-\mathbf{R}}{2} \quad \text{and} \quad \mathbf{P}_1 = \frac{\mathbf{P}}{2} + \frac{\mathbf{Q}+\mathbf{R}}{4} \tag{4.4}$$

Using the basis matrices defined in (3.13), (4.3) can be expressed concisely as

$$\left(\bar{\mathbf{P}} + \mathop{\mathbb{A}}_{i=1}^{\infty}\left\{\sum_{f\in\{-1,0,1\}} \mathbf{A}_f \otimes \mathbf{P}_f\right\}\right)\mathbf{U_e} = \mathbf{F_e}. \tag{4.5}$$

Note that (4.5) is identical to the PMDL system in (3.15) for $L_i = 1$ and $\mathbf{C_f} = \mathbf{P_f}$. Since the stiffness-preserving property of PMDL is independent of L_i, (3.15) with variable L_i is still an exact representation of the discrete half-space with respect to the stiffness at the interface with the interior at $x = 0$. Thus the discrete half-space can be replaced by PMDL elements with $\mathbf{C_f} = \mathbf{P_f}$. However, the PMDL system in (3.15) is still infinite. To make the computation tractable, it is truncated and a Dirichlet boundary condition applied at the end. The truncation introduces an error in the approximation of the discrete half-space. This can be handled by choosing complex values for L_i in a manner similar to PMDL. This will be discussed in more detail in Sec(4.3), where an error estimate for the boundary condition is derived.

To summarize, the exterior of the discrete lattice in (4.5) can be approximated in an efficient and accurate manner using the PMDL boundary conditions. This procedure to extend a continuum ABC to the discrete domain is the central idea of this thesis. This particular extension of PMDL to the discrete problem is named MD-PMDL. The details of the formulation of MD-PMDL for 1D is discussed in the subsequent sections.

4.1 MD-PMDL Formulation for 1D Lattice

Consider the governing equation for the exterior (including boundary cell) in (2.15),

$$\left(\mathop{\mathbb{A}}_{i=1}^{\infty} \left\{ \begin{bmatrix} p & q \\ r & p \end{bmatrix} \right\} + \bar{\mathbf{P}} \right) \mathbf{U_e} = \mathbf{F_e}. \tag{4.6}$$

It was shown in the previous sections that the operator on the left can be approximated using a truncated m layered PMDL system, i.e.,

$$\mathop{\mathbb{A}}_{i=1}^{\infty} \left\{ \begin{bmatrix} p & q \\ r & p \end{bmatrix} \right\} \mathbf{U_e} \approx \mathop{\mathbb{A}}_{i=1}^{m} \left\{ \frac{1}{L_i} c_{-1} \mathbf{A}_{-1} + c_0 \mathbf{A}_0 + L_i c_1 \mathbf{A}_1 \right\} \mathbf{U_e}, \tag{4.7}$$

where $\mathbf{A}_{-1}, \mathbf{A}_0$ and $\mathbf{A}_1$ are the basis matrices defined in (3.13) and the coefficients c_{-1}, c_0 and c_1 are given by:

$$c_{-1} = \frac{p}{2} - \frac{q+r}{4}, \quad c_0 = \frac{q-r}{2} \quad \text{and} \quad c_1 = \frac{p}{2} + \frac{q+r}{4}. \tag{4.8}$$

Note that $\mathbf{A}_{-1} = \mathbf{v}_{-1}\mathbf{v}_{-1}^t$ and $\mathbf{A}_1 = \mathbf{v}_1\mathbf{v}_1^t$, where $\mathbf{v}_{-1}^t = \begin{bmatrix} -1 & 1 \end{bmatrix}$ and $\mathbf{v}_1^t = \begin{bmatrix} 1 & 1 \end{bmatrix}$. Thus, (4.7) can be written as,

$$\left(\mathop{\mathbb{A}}_{i=1}^{m} \left\{ \frac{1}{L_i} c_{-1}\mathbf{v}_{-1}\mathbf{v}_{-1}^t + c_0\mathbf{A}_0 + L_i c_1 \mathbf{v}_1\mathbf{v}_1^t \right\} + \bar{\mathbf{P}} \right) \mathbf{U_e} = \mathbf{F_e}. \tag{4.9}$$

As mentioned in Sec(3), the lengths L_i in (4.9) are chosen to be complex to minimize the error in the approximation. This is discussed in more detail in Sec(4.3). Also, the imaginary part of L_i are made frequency dependent so that the equations are real valued when transformed back to time domain. Thus, the lengths are assumed to be of the form,

$$L_i = p_i + \frac{q_i}{\mathrm{i}\omega}, \quad i = 1, \ldots, m, \tag{4.10}$$

where p_i and q_i are parameters of the method that can be optimized to minimize the error in the approximation. Let us define state variables $s_{1,i}$ and $s_{2,i}$ for a unit cell i as,

$$\begin{aligned} s_{1,i} &= \frac{1}{L_i} c_{-1}\mathbf{v}_{-1}^t\mathbf{u}_i, \quad \text{and} \\ s_{2,i} &= L_i c_1 \mathbf{v}_1^t \mathbf{u}_i. \end{aligned} \tag{4.11}$$

The governing equation (4.9) can now be expressed in terms of the state variables as,

$$\mathop{\mathbb{A}}_{i=1}^{m} \left\{ \mathbf{v}_{-1}s_{1,i} + \mathbf{v}_1 s_{2,i} \right\} + \left(\mathop{\mathbb{A}}_{i=1}^{m} \left\{ c_0\mathbf{A}_0 \right\} + \bar{\mathbf{P}} \right) \mathbf{U_e} = \mathbf{F_e}. \tag{4.12}$$

Since L_i are frequency dependent, $\mathbf{s}_1$ and $\mathbf{s}_2$ are also frequency dependent, and can be derived by first substituting (4.10) into (4.11) and expanding:

$$\begin{aligned} p_i \left(\mathrm{i}\omega s_{1,i} \right) + q_i s_{1,i} &= c_{-1}\mathbf{v}_{-1}^t \left(\mathrm{i}\omega \mathbf{u}_i \right), \\ \left(\mathrm{i}\omega s_{2,i} \right) &= c_1 \mathbf{v}_1^t \left(p_i \left(\mathrm{i}\omega \mathbf{u_i} \right) + q_i \mathbf{u}_i \right). \end{aligned} \tag{4.13}$$

The time domain definition of state variables is obtained through an inverse fourier transform of (4.13) and is given by,

$$\begin{aligned} p_i \frac{\partial s_{1,i}}{\partial t} + q_i s_{1,i} &= c_{-1}\mathbf{v}_{-1}^t \frac{\partial \mathbf{u}_i}{\partial t}, \\ \frac{\partial s_{2,i}}{\partial t} &= c_1 \mathbf{v}_1^t \left(p_i \frac{\partial \mathbf{u}_i}{\partial t} + q_i \mathbf{u}_i \right). \end{aligned} \tag{4.14}$$

Equation (4.12) together with (4.14) is the complete statement of a m-layered MD-PMDL boundary condition for a 1D lattice and can summarized as

$$\begin{aligned} &\mathop{\mathbb{A}}_{i=1}^{m}\left\{\mathbf{v}_{-1}s_{1,i}+\mathbf{v}_1 s_{2,i}\right\}+\left(\mathop{\mathbb{A}}_{i=1}^{m}\left\{c_0\mathbf{A}_0\right\}+\bar{\mathbf{P}}\right)\mathbf{U_e}=\mathbf{F_e},\\ &\left.\begin{aligned} p_i\frac{\partial s_{1,i}}{\partial t}+q_i s_{1,i}&=c_{-1}\mathbf{v}_{-1}^t\frac{\partial \mathbf{u}_i}{\partial t}\\ \frac{\partial s_{2,i}}{\partial t}&=c_1\mathbf{v}_1^t\left(p_i\frac{\partial \mathbf{u}_i}{\partial t}+q_i\mathbf{u}_i\right)\end{aligned}\right\}\quad \text{for}\quad i=1,\ldots,m\,. \end{aligned} \tag{4.15}$$

4.2 Time Domain Implementation

The equations for the exterior at time $t=t_{n+1}$ can be written as:

$$\mathop{\mathbb{A}}_{i=1}^{m}\left\{\mathbf{v}_{-1}s_{1,i}^{n+1}+\mathbf{v}_1 s_{2,i}^{n+1}\right\}+\left(\mathop{\mathbb{A}}_{i=1}^{m}\left\{c_0\mathbf{A}_0\right\}+\bar{\mathbf{P}}\right)\mathbf{U_e}^{n+1}=\mathbf{F_e}^{n+1} \tag{4.16}$$

s_1^{n+1} and s_2^{n+1} can be obtained by discretizing (4.14) about $t=t_{n+\frac{1}{2}}$ using the Crank-Nicolson scheme, which is given by:

$$\begin{aligned} \frac{\partial(.)}{\partial t}^{n+\frac{1}{2}}&=\frac{(.)^{n+1}-(.)^n}{\Delta t}\,,\\ (.)^{n+\frac{1}{2}}&=\frac{(.)^{n+1}+(.)^n}{2}\,. \end{aligned} \tag{4.17}$$

Using (4.17) to discretize (4.14) results in the evolution equations for the state variables and are given by:

$$s_{1,i}^{n+1}=\frac{\hat{r_i}}{r_i}s_{1,i}^n+\frac{c_{-1}}{r_i}\mathbf{v}_{-1}^t\left(\mathbf{u}_i^{n+1}-\mathbf{u}_i^n\right), \tag{4.18}$$

$$s_{2,i}^{n+1}=s_{2,i}^n+c_1\mathbf{v}_1^t\left(r_i\mathbf{u}_i^{n+1}-\hat{r_i}\mathbf{u}_i^n\right), \tag{4.19}$$

where $r_i=p_i+q_i\frac{\Delta t}{2}$ and $\hat{r_i}=p_i-q_i\frac{\Delta t}{2}$. Substituting the expressions for the state variables (4.18) and (4.19) into (4.16), we obtain,

$$\begin{aligned} &\mathop{\mathbb{A}}_{i=1}^{m}\left\{\mathbf{v}_{-1}\frac{\hat{r_i}}{r_i}s_{1,i}^n\right\}+\left(\mathop{\mathbb{A}}_{i=1}^{m}\left\{\frac{c_{-1}}{r_i}\mathbf{v}_{-1}\mathbf{v}_{-1}^t\right\}\right)\left(\mathbf{U_e}^{n+1}-\mathbf{U_e}^n\right)+\\ &+\mathop{\mathbb{A}}_{i=1}^{m}\left\{\mathbf{v}_1 s_{2,i}^n\right\}+\left(\mathop{\mathbb{A}}_{i=1}^{m}\left\{c_1\mathbf{v}_1\mathbf{v}_1^t\right\}\right)\left(r_i\mathbf{U_e}^{n+1}-\hat{r}_i\mathbf{U_e}^n\right)\\ &+\left(\bar{\mathbf{P}}+\mathop{\mathbb{A}}_{i=1}^{m}\left\{c_0\mathbf{A}_0\right\}\right)\mathbf{U_e}^{n+1}=\mathbf{F_e^{n+1}}. \end{aligned} \tag{4.20}$$

The above equation can be rearranged and expressed as

$$\mathbf{K_L U_e}^{n+1} = \mathbf{F_e}^{n+1} + \mathbf{F_{sv}}^{n} + \mathbf{K_R U_e}^{n}, \tag{4.21}$$

where $\mathbf{K_L}$ and $\mathbf{K_R}$ are the stiffness matrices and $\mathbf{F_{sv}}$ is the forcing term due the state variables and are given by:

$$\begin{aligned}
\mathbf{K_L} &= \bar{\mathbf{P}} + \mathop{\mathbb{A}}_{i=1}^{m} \left\{ \frac{c_{-1}}{r_i}\mathbf{A}_{-1} + c_0\mathbf{A}_0 + r_i c_1 \mathbf{A}_1 \right\}, \\
\mathbf{K_R} &= \mathop{\mathbb{A}}_{i=1}^{m} \left\{ \frac{c_{-1}}{r_i}\mathbf{A}_{-1} + \hat{r_i} c_1 \mathbf{A}_1 \right\}, \\
\mathbf{F_{sv}}^{n} &= \mathop{\mathbb{A}}_{i=1}^{m} \left\{ \frac{\hat{r_i}}{r_i} s_{1,i}^{n} \mathbf{v}_{-1} + s_{2,i}^{n} \mathbf{v}_1 \right\}.
\end{aligned} \tag{4.22}$$

4.3 Derivation of an Error Estimate

Consider a general harmonic and periodic lattice governed by the equation,

$$\left(\mathop{\mathbb{A}}_{i=-\infty}^{\infty} \begin{bmatrix} \mathbf{A} & \mathbf{B} \\ \mathbf{C} & \mathbf{A} \end{bmatrix} \right) \mathbf{U} = \mathbf{F}. \tag{4.23}$$

The solution takes the form $\mathbf{u}_{n+\frac{1}{2}} = \sum_k \bar{\mathbf{u}}_k e^{ink}$, where k are the allowed wave modes that satisfy the governing equation (4.23). Substituting a single mode $\bar{u}_k e^{ink}$ in (4.23) results in,

$$\left(\mathbf{C}e^{-ik} + 2\mathbf{A} + \mathbf{B}e^{ik} \right) \bar{\mathbf{u}}_k = 0. \tag{4.24}$$

The relation (4.24) is also known as the dispersion relation.

The goal is to find the error in the approximation of the discrete half-space using MD-PMDL layers. Let us consider a wave mode traveling right in the interior and incident on the interface. If the exterior is an exact representation of the discrete half-space then the wave mode would travel into the exterior without causing any reflections at the interface. This is because the discrete half-space can only support outgoing wave modes. However, if the exterior is replaced by MD-PMDL layers, then the inexactness of the exterior would result in waves reflected into the interior. Thus the magnitude of the reflected wave compared to the incident wave could be taken as a quantitative measure of the error in the approximation of the discrete half-space.

Consider the solution field in the interior+boundary region ($i \leq \frac{1}{2}$) as,

$$\mathbf{u}_{n+\frac{1}{2}} = \mathbf{I}e^{ink_1} + R\,\mathbf{I}e^{ink_2} \quad \text{for} \quad n \leq 0, \tag{4.25}$$

where k_1 is forward propagating wave number, k_2 is the backward propagating wave number, $\mathbf{I}$ is the amplitude of the incident wave mode and $R\,\mathbf{I}$ is the magnitude of the reflected wave. The scalar R, which is the ratio of the the reflected mode to the incident mode is known as the Reflection Coefficient. Note that $R = 1$ if the wave is completely reflected at the interface and $R = 0$ if it is completely absorbed. Thus, a low value of R implies a good approximation of the discrete half-space.

The incident and the reflected modes should satisfy the dispersion relation, i.e.,

$$\left(\mathbf{C}e^{-ik_1} + 2\mathbf{A} + \mathbf{B}e^{ik_1}\right)\mathbf{I} = 0, \tag{4.26}$$

$$R\left(\mathbf{C}e^{-ik_2} + 2\mathbf{A} + \mathbf{B}e^{ik_2}\right)\mathbf{I} = 0. \tag{4.27}$$

Subtracting (4.26) from (4.27) and simplifying, we get:

$$\begin{aligned} &\left(e^{k_1} - e^{k_2}\right)\left(\mathbf{C}e^{-k_1}e^{-k_2} - \mathbf{B}\right)\mathbf{I} = 0, \\ &\implies \mathbf{B}e^{k_1}\mathbf{I} = \mathbf{C}e^{-k_2}\mathbf{I} \quad \text{for} \quad k_1 \neq k_2. \end{aligned} \tag{4.28}$$

Substituting (4.28) into (4.26), we get:

$$\left(\mathbf{C}e^{-k_2} + \mathbf{A}\right)\mathbf{I} = -\left(\mathbf{C}e^{-k_1} + \mathbf{A}\right)\mathbf{I}. \tag{4.29}$$

Now consider the boundary cell, i.e $n = 0$. The governing equation for the cell can be written as,

$$\begin{bmatrix} \mathbf{A} & \mathbf{B} \\ \mathbf{C} & \mathbf{A} \end{bmatrix} \begin{Bmatrix} \mathbf{u}_{-\frac{1}{2}} \\ \mathbf{u}_{\frac{1}{2}} \end{Bmatrix} = \begin{Bmatrix} \mathbf{f}_{-\frac{1}{2}} \\ \mathbf{f}_{\frac{1}{2}} \end{Bmatrix}. \tag{4.30}$$

Using the definition of the half-space stiffness (2.17), i.e $\mathbf{f}_{\frac{1}{2}} = \mathbf{K_{approx}}\mathbf{u}_{\frac{1}{2}}$, and substituting (4.25) into second equation of (4.30), we get:

$$\begin{aligned} &\mathbf{C}\left(\mathbf{I}e^{-ik_1} + R\mathbf{I}e^{-ik_2}\right) + \mathbf{A}\left(\mathbf{I} + R\mathbf{I}\right) = \mathbf{K_{approx}}\left(\mathbf{I} + R\mathbf{I}\right), \\ &\implies R\left(\mathbf{C}e^{-ik_2} + \mathbf{A}\right)\mathbf{I} + \left(\mathbf{A} + \mathbf{C}e^{-ik_1}\right)\mathbf{I} = \mathbf{K_{approx}}\left(1 + R\right)\mathbf{I}. \end{aligned} \tag{4.31}$$

Note that if the half-space was exact then $R = 0$ and (4.31) yields:

$$(\mathbf{C}e^{-ik_1} + \mathbf{A})\mathbf{I} = \mathbf{K_{exact}}\mathbf{I}. \tag{4.32}$$

Using (4.29) and (4.32), (4.31) can be simplified to:

$$\begin{aligned} &(1 - R)(\mathbf{C}e^{-k_1} + \mathbf{A})\mathbf{I} = (1 + R)\mathbf{K_{approx}}\mathbf{I} \\ &\implies (1 - R)\mathbf{K_{exact}}\mathbf{I} = (1 + R)\mathbf{K_{approx}}\mathbf{I}. \end{aligned} \tag{4.33}$$

Thus, we finally obtain a relation for the Reflection Coefficient R given by:

$$\det((1-R)\mathbf{K_{exact}} - (1+R)\mathbf{K_{approx}}) = 0. \tag{4.34}$$

Error Estimate for 1D MD-PMDL

For the 1-D case, Reflection Coefficient in (4.34) can be written as,

$$R = \left| \frac{K_{exact} - K_{approx}}{K_{exact} + K_{approx}} \right|. \tag{4.35}$$

Also, the equation of the exterior for the general lattice, (2.15) is given by:

$$\left(\overset{\infty}{\underset{i=1}{\mathbb{A}}} \begin{bmatrix} p & q \\ r & p \end{bmatrix} \right) \mathbf{U} = \mathbf{F}, \tag{4.36}$$

where p, q and r are scalars. It can be easily shown that the the exact half-space stiffness for the above system is given by $K_{exact}^2 = p^2 - qr$.

Assuming n MD-PMDL cells are used in the approximation of the exterior, i.e :

$$\left(\overset{\infty}{\underset{i=1}{\mathbb{A}}} \begin{bmatrix} p & q \\ r & p \end{bmatrix} \right) \approx \left(\overset{n}{\underset{i=1}{\mathbb{A}}} \begin{bmatrix} a_i & b_i \\ c_i & a_i \end{bmatrix} \right) \tag{4.37}$$

where,

$$\begin{aligned} a_i &= \frac{1}{2}\left(p - \frac{q+r}{2}\right)\frac{1}{L_i} + \frac{1}{2}\left(p + \frac{q+r}{2}\right)L_i, \\ b_i &= -\frac{1}{2}\left(p - \frac{q+r}{2}\right)\frac{1}{L_i} + \frac{1}{2}(q-r) + \frac{1}{2}\left(p + \frac{q+r}{2}\right)L_i \quad \text{and} \\ c_i &= -\frac{1}{2}\left(p - \frac{q+r}{2}\right)\frac{1}{L_i} - \frac{1}{2}(q-r) + \frac{1}{2}\left(p + \frac{q+r}{2}\right)L_i. \end{aligned} \tag{4.38}$$

If K_n is the stiffness of the n-cell MD-PMDL exterior, then the reflection coefficient is given by

$$R_n = \left| \frac{K_{exact} - K_n}{K_{exact} + K_n} \right|. \tag{4.39}$$

Note that a_i and b_i have the property

$$a_i^2 - b_i c_i = K_{exact}^2. \tag{4.40}$$

Also, since PMDL is a rational approximation of the half-space (3.8), we can write,

$$K_i = a_i - \frac{b_i c_i}{a_i + K_{i-1}}. \tag{4.41}$$

Note that if K_{j-1} is exact, i.e $K_{j-1} = K_{exact}$, then we recover back the exact half-space stiffness from (4.41), i.e $K_i = K_{exact}$. Substituting (4.41) into (4.39) and using (4.40) to simplify, we get a recursive definition for reflection coefficient, i.e.:

$$\begin{aligned} R_n &= \left| \frac{(a_n - K_{exact})\,(K_{exact} - K_{n-1})}{(a_n + K_{exact})\,(K_{exact} + K_{n-1})} \right| \\ &= \left| \frac{(a_n - K_{exact})}{(a_n + K_{exact})} \right| R_{n-1}. \end{aligned} \tag{4.42}$$

Since, the layers are truncated with a fixed boundary condition we set $K_0 = \infty$. Thus the reflection coefficient can be written explicitly as:

$$R_n = \prod_{i=1}^{n} \left| \frac{a_i - K_{exact}}{a_i + K_{exact}} \right| . \tag{4.43}$$

If K_{exact} is imaginary(propagating modes) and L is real, then $R = 1$ and hence the wave mode will be completely reflected. Thus to prevent reflection L_i should be chosen complex. Similarly, if K_{exact} is real(evanescent wave modes) then L_i has to be real. This is the reason for choosing the general complex form in (4.10) for the lengths L_i.

Since the aim of MD-PMDL is to be minimize the reflections, the lengths L_i should be chosen such that R is close to 0. Note that since each term is smaller than 1, the product goes to zero exponentially with the number of layers. Thus, the error decays exponentially with the number of MD-PMDL layers. We could optimize the number of layers by choosing optimal values for parameters L_i such that R is minimized. However, ad-hoc values of L_i are used for the simulations in this work and optimization of the parameters is a topic for future study.

4.3.1 A comparison of the error estimates between PMDL and MD-PMDL for the Discrete Wave Equation

Consider the exterior for the 1D discrete wave equation in (2.3) and for simplicity assume $a = h$, $b = hk_x^2$ and $f = 0$, i.e.,

$$-D_x^2 u_{j+\frac{1}{2}} - k_x^2 u_{j+\frac{1}{2}} = 0, \quad j = 0, .., \infty \tag{4.44}$$

or, the equivalent assembly:

$$\left(\mathop{\mathbb{A}}_{i=1}^{\infty} \begin{bmatrix} \frac{1}{h} - \frac{k_x^2 h}{2} & -\frac{1}{h} \\ -\frac{1}{h} & \frac{1}{h} - \frac{k_x^2 h}{2} \end{bmatrix} \right) \mathbf{u_e} = \mathbf{f_e}. \tag{4.45}$$

The MD-PMDL approximation for (4.45) can be written as,

$$\begin{aligned}
&\left(\mathop{\mathbb{A}}_{i=1}^{n}\begin{bmatrix}\bar{a}_i & \bar{b}_i\\ \bar{b}_i & \bar{a}_i\end{bmatrix}\right)\mathbf{u_e}=\mathbf{f_e}, \quad \text{where}\\
&\bar{a}_i=\left(\frac{1}{h}-\frac{k_x^2h}{4}\right)\frac{1}{L_i}-k_x^2h\frac{L_i}{4}\\
&\bar{b}_i=-\left(\frac{1}{h}-\frac{k_x^2h}{4}\right)\frac{1}{L_i}-k_x^2h\frac{L_i}{4}.
\end{aligned} \tag{4.46}$$

Also from (4.24), the dispersion relation for (4.45) is given by:

$$\begin{aligned}
&\frac{1}{h}\left(e^{-ikh}-2+e^{ikh}\right)=k_x^2h\\
&\implies \sin^2\frac{kh}{2}=\frac{k_x^2h^2}{4}.
\end{aligned} \tag{4.47}$$

As seen earlier, the discrete half-space stiffness is given by:

$$\begin{aligned}
K_{exact}^{disc}&=\sqrt{\left(\frac{1}{h}-\frac{k_x^2h}{2}\right)^2-\left(\frac{1}{h}\right)^2}\\
&=-i\sqrt{k_x^2\left(1-\frac{k_x^2h^2}{4}\right)}.
\end{aligned} \tag{4.48}$$

Using (4.47), (4.48) can be simplified to

$$K_{exact}^{disc}=-\frac{i}{h}\sin\left(kh\right),. \tag{4.49}$$

and substituting (4.49) and (4.46) in (4.43), we get the reflection coefficient as:

$$R_n^{md-pmdl}=\prod_{j=1}^{n}\left|\frac{ih-L_j\tan\left(\frac{kh}{2}\right)}{ih+L_j\tan\left(\frac{kh}{2}\right)}\right|^2. \tag{4.50}$$

We now derive the reflection coefficient when PMDL is used for the right exterior. The reflection coefficient when PMDL is used for the right exterior is given by:

$$R_n^{pmdl}=\frac{K_{exact}^{disc}-K_{pmdl}}{K_{exact}^{disc}+K_{pmdl}}, \tag{4.51}$$

where, K_{pmdl} is the stiffness of the PMDL layers formulated for the system obtained as the continuum limit ($h\to 0$) of the discrete wave equation. i.e.,

$$-\frac{\partial^2u}{\partial x^2}-k_x^2u=f. \tag{4.52}$$

The Reflection Coefficient when PMDL is used to approximate the continuous half-space stiffness of (4.52) is given by:

$$R_n^{cont} = \frac{K_{exact}^{cont} - K_{pmdl}}{K_{exact}^{cont} + K_{pmdl}} \tag{4.53}$$

where $K_{exact}^{cont} = -ik_x$ is the continuous half-space stiffness. Using (4.53), the stiffness of the PMDL layers can be written as,

$$K_{pmdl} = \alpha K_{exact}^{cont}, \quad \text{where} \quad \alpha = \frac{1 - R_n^{cont}}{1 + R_n^{cont}}. \tag{4.54}$$

Finally, substituting (4.54) into (4.51), we get:

$$R_n^{continuous-pmdl} = \frac{K_{exact}^{disc} - \alpha K_{exact}^{cont}}{K_{exact}^{disc} + \alpha K_{exact}^{cont}}. \tag{4.55}$$

Substituting the expressions for the half-space stiffnesses, (4.55) can be further simplified to:

$$R_n^{continuous-pmdl} = \frac{\cos\left(\frac{kh}{2}\right) - \alpha}{\cos\left(\frac{kh}{2}\right) + \alpha}. \tag{4.56}$$

Thus (4.50) and (4.56) are the error measures when MD-PMDL and Continuous PMDL are used to approximate the right exterior and are plotted in Fig.(4.1). The Reflection coefficients are plotted against normalized horizontal wave-numbers (kh) for a set of parameters ($L_i's$) that were chosen in an ad-hoc fashion. The plot shows that at low wave-numbers the Reflection Coefficients are equal for PMDL and MD-PMDL. However, for high wave-numbers MD-PMDL performs much better than PMDL which does not improve even with a large number of layers. This justifies our initial claim that continuum ABC's cannot be directly used to approximate discrete systems. We will now present some numerical results that shows the effectiveness of MD-PMDL.

4.4 Numerical Experiment: 1D Discrete Wave Equation

The wave equation for a discrete half-space ($x \geq 0$) is given by:

$$-a_x D_x^2 u(x,t) + \frac{\partial^2 u(x,t)}{\partial t^2} = 0 \tag{4.57}$$

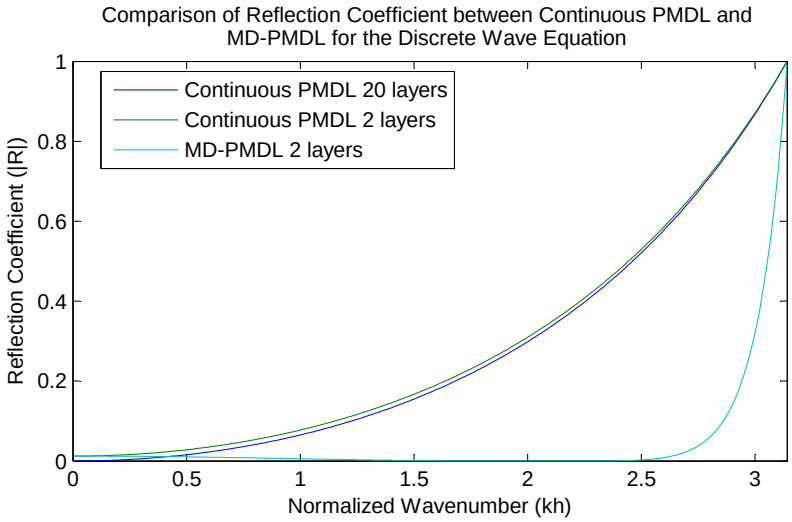

Figure 4.1: Plot of the Reflection Coefficient when continuous PMDL and MD-PMDL boundary conditions are used for the Discrete Wave Equation.

The domain of interest is chosen to be n(=10) atoms with positions $x_j = (j-1) * h, j = 1, 2, .., 10$ where h is the lattice spacing. The initial and the loading condition are given by:

$$f(0,t) = \begin{cases} \sin^2(\frac{\pi}{2}t) & t < 2\pi \\ 0 & \text{otherwise} \end{cases} \tag{4.58}$$

$$u(x,0) = 0 \tag{4.59}$$

$$\dot{u}(x,0) = 0 \tag{4.60}$$

The velocity norm is used as the criteria to compare the different boundary conditions, as it provides a measure of the total KE of the system and hence the temperature. The simulation is performed using MD-PMDL and continuous PMDL to approximate the discrete half-space. 3 layers of MD-PMDL were used with parameters $\{(p_i, q_i) = (0, \frac{1}{16}), (0, \frac{4}{16}), (0, \frac{9}{16})\}$, and the same parameters are used for the PMDL boundary conditions. Note that the parameters were chosen in an ad-hoc manner. The results are compared with the exact solution which is computed by using a much larger domain (1000 atoms) so that the boundary effects are not seen in the region of interest.

The relative errors from the two simulations are shown in Fig(4.2). As expected, Continuous PMDL has significant errors(10%) while MD-PMDL has a much smaller error(0.2%).

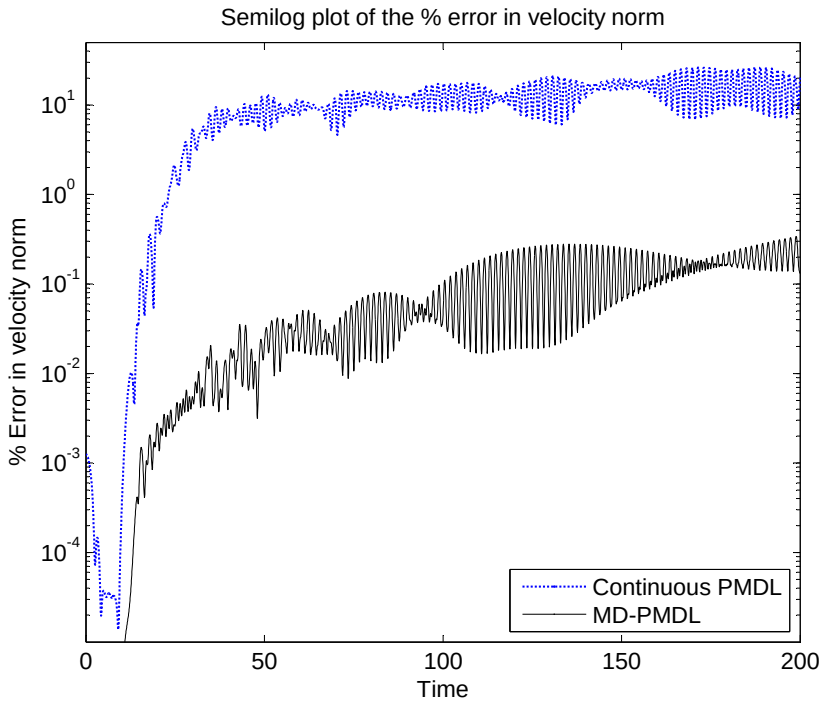

Figure 4.2: A semilog plot of the relative error in velocity norm over the duration of the simulation.

Chapter 5

MD-PMDL Formulation for 2D Square Lattice

Similar to the 1-D case, the governing equation for a periodic square lattice can be written in terms of the basis matrices defined in (3.13) as:

$$\underset{\substack{i=-\infty,..,\infty \\ j=-\infty,..,\infty}}{\mathbb{A}} \left\{ \sum_{\substack{f\in\{-1,0,1\} \\ g\in\{-1,0,1\}}} c_{f,g} \mathbf{A_f} \otimes \mathbf{A_g} \right\} \mathbf{U} = \mathbf{F}, \tag{5.1}$$

where $c_{f,g}$ are constants that can be determined from harmonic approximation of the system. The 2-D assembly on the left hand side of (5.1) can be rewritten as a 1-D assembly given by:

$$\overset{\infty}{\underset{i=-\infty}{\mathbb{A}}} \left\{ \sum_{f\in\{-1,0,1\}} \mathbf{A_f} \otimes \mathbf{O}_f \right\}, \tag{5.2}$$

where,

$$\mathbf{O}_f = \overset{\infty}{\underset{j=-\infty}{\mathbb{A}}} \left\{ \sum_{g\in\{-1,0,1\}} c_{f,g} \mathbf{A_g} \right\}. \tag{5.3}$$

Note that the assembly in (5.2) is exactly the same as in (4.5), and hence can be rewritten (similar to the 1-D case) using the equivalent assembly in (3.15) as:

$$\overset{\infty}{\underset{i=-\infty}{\mathbb{A}}} \left\{ \sum_{f\in\{-1,0,1\}} L_i^f \mathbf{A_f} \otimes \mathbf{O}_f \right\}. \tag{5.4}$$

Substituting back $\mathbf{O}_f$ from (5.3) into (5.4), we get:

$$\underset{\substack{i=-\infty,..,\infty \\ j=-\infty,..,\infty}}{\mathbb{A}} \left\{ \sum_{\substack{f\in\{-1,0,1\} \\ g\in\{-1,0,1\}}} c_{f,g} L_i^f \mathbf{A_f} \otimes \mathbf{A_g} \right\}. \tag{5.5}$$

This procedure can be repeated in a similar fashion for the assembly along y direction to get:

$$\underset{\substack{i=-\infty,..,\infty \\ j=-\infty,..,\infty}}{\mathbb{A}} \left\{ \sum_{\substack{f\in\{-1,0,1\} \\ g\in\{-1,0,1\}}} c_{f,g} L_i^f L_j^g \mathbf{A_f} \otimes \mathbf{A_g} \right\}. \tag{5.6}$$

The assembly in (5.6) is the final form of PMDL lattice that is equivalent (with respect to stiffness) to the original system and has exact stiffness matching property at any interface irrespective of the spacings L_i and L_j. Note that for the choice of $L_i = 1$ and $L_j = 1$, (5.6) is identical to the original matrix operator in (5.1).

Similar to the decomposition in the 1-D lattice, the 2-D lattice can also be split into an interior and an exterior system that are coupled by the boundary region, i.e.,

$$\begin{aligned} \mathbf{A_{ii}U_i} &= \mathbf{F_i} - \mathbf{A_{ie}U_e}, \\ \mathbf{A_{ee}U_e} &= \mathbf{F_e} - \mathbf{A_{ei}U_i}. \end{aligned} \tag{5.7}$$

Note that the interior is coupled with the exterior only along the boundary and the treatment of the interior is exactly the same as in the 1-D case and thus only the treatment of the exterior will be discussed here. Note that the exterior can be viewed as an assembly of 3 super cell's(see Fig.5.1(b)) $\mathbf{E_x}, \mathbf{E_y}$ and $\mathbf{C_{xy}}$, i.e.

$$\mathbf{A_{ee}U_e} = \left(\bar{\mathbf{P}} + \mathbb{A}\left\{\mathbf{E_x}, \mathbf{E_y}, \mathbf{C_{xy}}\right\}\right) \mathbf{U_e}. \tag{5.8}$$

The super cells $\mathbf{E_x}$ and $\mathbf{E_y}$ will be referred to as edge exteriors as they extend to $+\infty$ along x and y respectively. Similarly the super cell $\mathbf{C_{xy}}$ will be referred to as the corner exterior as it extends to $+\infty$ along both x and y directions. The system of equations for the super-cells

is given by:

$$\mathbf{E_x} = \underset{\substack{i=1,..,\infty \\ j=-\infty,..,-1}}{\mathbb{A}} \left\{ \sum_{\substack{f\in\{-1,0,1\} \\ g\in\{-1,0,1\}}} c_{f,g} L_i^f \mathbf{A_f} \otimes \mathbf{A_g} \right\},$$

$$\mathbf{E_y} = \underset{\substack{i=-\infty,..,-1 \\ j=1,..,\infty}}{\mathbb{A}} \left\{ \sum_{\substack{f\in\{-1,0,1\} \\ g\in\{-1,0,1\}}} c_{f,g} L_j^g \mathbf{A_f} \otimes \mathbf{A_g} \right\}, \tag{5.9}$$

$$\mathbf{C_{xy}} = \underset{\substack{i=1,..,\infty \\ j=1,..,\infty}}{\mathbb{A}} \left\{ \sum_{\substack{f\in\{-1,0,1\} \\ g\in\{-1,0,1\}}} c_{f,g} L_i^f L_j^g \mathbf{A_f} \otimes \mathbf{A_g} \right\}.$$

We now need to truncate $\mathbf{E_x}$ along x and $\mathbf{E_y}$ along y and $\mathbf{C_{xy}}$ along both x and y. Again, similar to the 1-D case, the truncated system can be written as:

$$\mathbf{E_x} = \underset{\substack{i=1,..,m_x \\ j=-\infty,..,-1}}{\mathbb{A}} \left\{ \sum_{\substack{f\in\{-1,0,1\} \\ g\in\{-1,0,1\}}} c_{f,g} L_i^f \mathbf{A_f} \otimes \mathbf{A_g} \right\},$$

$$\mathbf{E_y} = \underset{\substack{i=-\infty,..,-1 \\ j=1,..,m_y}}{\mathbb{A}} \left\{ \sum_{\substack{f\in\{-1,0,1\} \\ g\in\{-1,0,1\}}} c_{f,g} L_j^g \mathbf{A_f} \otimes \mathbf{A_g} \right\}, \tag{5.10}$$

$$\mathbf{C_{xy}} = \underset{\substack{i=1,..,m_x \\ j=1,..,m_y}}{\mathbb{A}} \left\{ \sum_{\substack{f\in\{-1,0,1\} \\ g\in\{-1,0,1\}}} c_{f,g} L_i^f L_j^g \mathbf{A_f} \otimes \mathbf{A_g} \right\}.$$

Note that the unit cell of $\mathbf{C_{xy}}$ reduces to that of $\mathbf{E_x}$ and $\mathbf{E_y}$ for $L_j = 1$ and $L_i = 1$ respectively. Thus, the formulation for $\mathbf{C_{xy}}$ is derived first and the formulations for $\mathbf{E_y}$ and $\mathbf{E_x}$ can then be obtained as a special case of the corner formulation.

5.1 Formulation for the Corner Exterior

The system of equations for the corner region $\mathbf{C_{xy}}$ are given by:

$$\underset{\substack{i=1,..,m_x \\ j=1,..,m_y}}{\mathbb{A}} \left\{ \sum_{\substack{f\in\{-1,0,1\} \\ g\in\{-1,0,1\}}} c_{f,g} L_i^f L_j^g \mathbf{A_f} \otimes \mathbf{A_g} \right\} \mathbf{U_c} = \mathbf{F_c}. \tag{5.11}$$

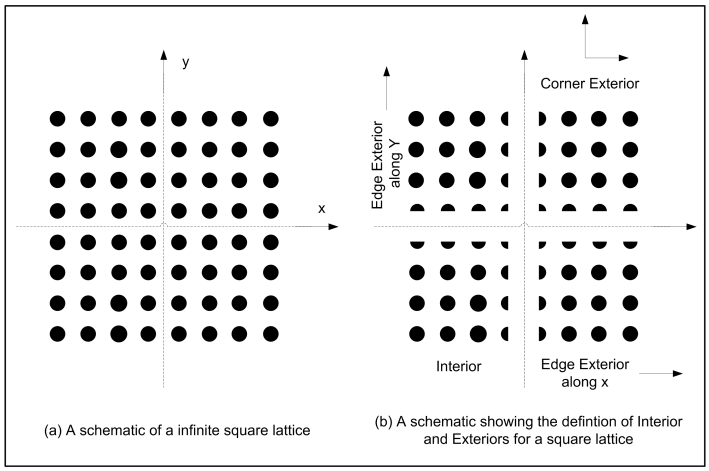

Figure 5.1: A schematic of an infinite square lattice.

Recall that the basis matrices can be decomposed as

$$\mathbf{A_{-1}} = \mathbf{v_{-1}}\mathbf{v_{-1}^t}, \quad \mathbf{A_0} = \mathbf{v_1}\mathbf{v_{-1}^t} \quad \text{and} \quad \mathbf{A_1} = \mathbf{v_1}\mathbf{v_1^t} \tag{5.12}$$

where $\mathbf{v_{-1}^t} = \begin{bmatrix} -1 & 1 \end{bmatrix}$ and $\mathbf{v_1^t} = \begin{bmatrix} 1 & 1 \end{bmatrix}$. Based on (5.12), Kronecker product of any two basis matrix can be represented as

$$\begin{aligned} \mathbf{A_i} \otimes \mathbf{A_j} &= \left(\mathbf{a_1}\mathbf{a_2^t}\right) \otimes \left(\mathbf{b_1}\mathbf{b_2^t}\right) \\ &= \left(\mathbf{a_1} \otimes \mathbf{b_1}\right) \left(\mathbf{a_2} \otimes \mathbf{b_2}\right)^{\mathbf{t}} \end{aligned} \tag{5.13}$$

Using (5.13) and (5.12), we can rewrite (5.11) as

$$\underset{\substack{i=1,..,m_x \\ j=1,..,m_y}}{\mathbb{A}} \left\{ \begin{array}{l} \left(\mathbf{v_{-1}} \otimes \mathbf{v_{-1}}\right) s_{1,(i,j)} + \left(\mathbf{v_{-1}} \otimes \mathbf{v_1}\right) s_{2,(i,j)} + \\ + \left(\mathbf{v_1} \otimes \mathbf{v_{-1}}\right) s_{3,(i,j)} + \left(\mathbf{v_1} \otimes \mathbf{v_1}\right) s_{4,(i,j)} + \\ + c_{0,0} \left(\mathbf{A_0} \otimes \mathbf{A_0}\right) \mathbf{u_{i,j}} \end{array} \right\} = \mathbf{F_c}, \tag{5.14}$$

where $\mathbf{s_1}, \mathbf{s_2}, \mathbf{s_3}$ and $\mathbf{s_4}$ are the state variables for the corner region and are given by

$$\begin{aligned} s_{1,(i,j)} &= \frac{c_{-1,-1}}{L_i L_j} \left(\mathbf{v_{-1}} \otimes \mathbf{v_{-1}}\right)^{\mathbf{t}} \mathbf{u_{i,j}}, \\ s_{2,(i,j)} &= \frac{c_{-1,0}}{L_i} \left(\mathbf{v_{-1}} \otimes \mathbf{v_{-1}}\right)^{\mathbf{t}} \mathbf{u_{i,j}} + \frac{c_{-1,1} L_j}{L_i} \left(\mathbf{v_{-1}} \otimes \mathbf{v_1}\right)^{\mathbf{t}} \mathbf{u_{i,j}}, \\ s_{3,(i,j)} &= \frac{c_{0,-1}}{L_j} \left(\mathbf{v_{-1}} \otimes \mathbf{v_{-1}}\right)^{\mathbf{t}} \mathbf{u_{i,j}} + \frac{c_{1,-1} L_i}{L_j} \left(\mathbf{v_1} \otimes \mathbf{v_{-1}}\right)^{\mathbf{t}} \mathbf{u_{i,j}}, \\ s_{4,(i,j)} &= c_{0,1} L_j \left(\mathbf{v_{-1}} \otimes \mathbf{v_1}\right)^{\mathbf{t}} \mathbf{u_{i,j}} + c_{1,0} L_i \left(\mathbf{v_1} \otimes \mathbf{v_{-1}}\right)^{\mathbf{t}} \mathbf{u_{i,j}}, \\ &\quad + c_{1,1} L_i L_j \left(\mathbf{v_1} \otimes \mathbf{v_1}\right)^{\mathbf{t}} \mathbf{u_{i,j}}. \end{aligned} \tag{5.15}$$

Once the state variables are defined, the derivation is identical to the 1D derivation. Thus (5.15) are inverse fourier transformed to obtain the time domain equations for the state variables which are then discretized using the Crank-Nicolson method to obtain the evolution equations for the state variables. These evolution equations are given by

$$\begin{aligned} s^{n+1}_{1,(i,j)} &= \frac{\hat{r}_i}{r_i} s^n_{1,(i,j)} + \frac{1}{r_i}\left(\hat{s}^{n+1}_{1,(i,j)} - \hat{s}^n_{1,(i,j)}\right), \\ \hat{s}^{n+1}_{1,(i,j)} &= \frac{\hat{r}_j}{r_j} \hat{s}^n_{1,(i,j)} + \frac{c_{-1,-1}}{r_j}\left(\mathbf{v_{-1}} \otimes \mathbf{v_{-1}}\right)^{\mathbf{t}} \left(\mathbf{u_{i,j}}^{n+1} - \mathbf{u_{i,j}}^n\right), \end{aligned} \tag{5.16}$$

$$\begin{aligned} s^{n+1}_{2,(i,j)} = \frac{\hat{r}_i}{r_i} s^n_{2,(i,j)} &+ \frac{c_{-1,0}}{r_i}\left(\mathbf{v_{-1}} \otimes \mathbf{v_{-1}}\right)^{\mathbf{t}} \left(\mathbf{u_{i,j}}^{n+1} - \mathbf{u_{i,j}}^n\right) + \\ &\frac{c_{-1,1}}{r_i}\left(\mathbf{v_{-1}} \otimes \mathbf{v_1}\right)^{\mathbf{t}} \left(r_j \mathbf{u_{i,j}}^{n+1} - \hat{r}_j \mathbf{u_{i,j}}^n\right), \end{aligned} \tag{5.17}$$

$$\begin{aligned} s^{n+1}_{3,(i,j)} = \frac{\hat{r}_j}{r_j} s^n_{3,(i,j)} &+ \frac{c_{0,-1}}{r_j}\left(\mathbf{v_{-1}} \otimes \mathbf{v_{-1}}\right)^{\mathbf{t}} \left(\mathbf{u_{i,j}}^{n+1} - \mathbf{u_{i,j}}^n\right) + \\ &\frac{c_{1,-1}}{r_j}\left(\mathbf{v_1} \otimes \mathbf{v_{-1}}\right)^{\mathbf{t}} \left(r_i \mathbf{u_{i,j}}^{n+1} - \hat{r}_i \mathbf{u_{i,j}}^n\right) \end{aligned} \tag{5.18}$$

$$\begin{aligned} s^{n+1}_{4,(i,j)} = s^n_{4,(i,j)} &+ c_{0,1}\left(\mathbf{v_{-1}} \otimes \mathbf{v_1}\right)^{\mathbf{t}} \left(r_j \mathbf{u_{i,j}}^{n+1} - \hat{r}_j \mathbf{u_{i,j}}^n\right) + \\ &c_{1,0}\left(\mathbf{v_1} \otimes \mathbf{v_{-1}}\right)^{\mathbf{t}} \left(r_i \mathbf{u_{i,j}}^{n+1} - \hat{r}_i \mathbf{u_{i,j}}^n\right) + \\ &\left(r_i \hat{s}^{n+1}_{4,(i,j)} - \hat{r}_i \hat{s}^n_{4,(i,j)}\right), \\ \hat{s}^{n+1}_{4,(i,j)} = \hat{s}^n_{4,(i,j)} &+ c_{1,1}\left(\mathbf{v_1} \otimes \mathbf{v_1}\right)^{\mathbf{t}} \left(r_j \mathbf{u_{i,j}}^{n+1} - \hat{r}_j \mathbf{u_{i,j}}^n\right). \end{aligned} \tag{5.19}$$

Substituting (5.16), (5.17), (5.18) and (5.19) into (5.14) evaluated at $t = t_{n+1}$, we get the final system of equations for the corner exterior as

$$\mathbf{K_{L,c_{xy}}} \mathbf{U^{n+1}_{c_{xy}}} = \mathbf{F^{n+1}_{c_{xy}}} + \mathbf{F^{n}_{sv,c_{xy}}} + \mathbf{K_{R,c_{xy}}} \mathbf{U^{n}_{c_{xy}}}, \tag{5.20}$$

where $\mathbf{F_{c_{xy}}}$ is the coupling force with the edge exteriors, $\mathbf{K_{L,c_{xy}}}$ and $\mathbf{K_{R,c_{xy}}}$ are the stiffness matrices and $\mathbf{F_{sv,c_{xy}}}$ is the force term from the state variables. The explicit expressions for these are given by

$$\mathbf{K_{L,c_{xy}}} = \underset{\substack{i=1,..,m_x \\ j=1,..,m_y}}{\mathbb{A}} \left\{ \begin{array}{l} \frac{c_{-1,-1}}{r_i r_j}\mathbf{A_{-1}} \otimes \mathbf{A_{-1}} + \frac{c_{-1,0}}{r_i}\mathbf{A_{-1}} \otimes \mathbf{A_0} + \frac{c_{-1,1} r_j}{r_i}\mathbf{A_{-1}} \otimes \mathbf{A_1} + \\ + \frac{c_{0,-1}}{r_j}\mathbf{A_0} \otimes \mathbf{A_{-1}} + c_{0,0}\mathbf{A_0} \otimes \mathbf{A_0} + c_{0,1} r_j \mathbf{A_0} \otimes \mathbf{A_1} + \\ + \frac{c_{1,-1} r_i}{r_j}\mathbf{A_1} \otimes \mathbf{A_{-1}} + c_{1,0} r_i \mathbf{A_1} \otimes \mathbf{A_0} + c_{1,1} r_i r_j \mathbf{A_1} \otimes \mathbf{A_1} \end{array} \right\}, \quad (5.21)$$

$$\mathbf{K_{R,c_{xy}}} = \underset{\substack{i=1,..,m_x \\ j=1,..,m_y}}{\mathbb{A}} \left\{ \begin{array}{l} \frac{c_{-1,-1}}{r_i r_j}\mathbf{A_{-1}} \otimes \mathbf{A_{-1}} + \frac{c_{-1,0}}{r_i}\mathbf{A_{-1}} \otimes \mathbf{A_0} + \frac{c_{-1,1} \hat{r}_j}{r_i}\mathbf{A_{-1}} \otimes \mathbf{A_1} + \\ + \frac{c_{0,-1}}{r_j}\mathbf{A_0} \otimes \mathbf{A_{-1}} + c_{0,1} \hat{r}_j \mathbf{A_0} \otimes \mathbf{A_1} + \\ + \frac{c_{1,-1} \hat{r}_i}{r_j}\mathbf{A_1} \otimes \mathbf{A_{-1}} + c_{1,0} \hat{r}_i \mathbf{A_1} \otimes \mathbf{A_0} + c_{1,1} r_i \hat{r}_j \mathbf{A_1} \otimes \mathbf{A_1} \end{array} \right\}, \quad (5.22)$$

$$\mathbf{F^n_{sv,c_{xy}}} = \underset{\substack{i=1,..,m_x \\ j=1,..,m_y}}{\mathbb{A}} \left\{ \begin{array}{l} \mathbf{v_{-1}} \otimes \mathbf{v_{-1}} \left[\frac{\hat{r}_i}{r_i} s^n_{1,(i,j)} + \frac{\hat{r}_j}{r_i r_j} \hat{s}^n_{1,(i,j)} \right] + \\ + \mathbf{v_{-1}} \otimes \mathbf{v_1} \frac{\hat{r}_i}{r_i} s^n_{2,(i,j)} + \mathbf{v_1} \otimes \mathbf{v_{-1}} \frac{\hat{r}_j}{r_j} s^n_{3,(i,j)} + \\ + \mathbf{v_1} \otimes \mathbf{v_1} \left[s^n_{4,(i,j)} + (r_i - \hat{r}_i)\, \hat{s}^n_{4,(i,j)} \right] \end{array} \right\}. \quad (5.23)$$

5.2 Formulation for Edge Exteriors

The state variables for the edge exterior along x, $\mathbf{E_x}$, can be obtained from by setting $L_j = 1$ in (5.15) and are given by

$$\begin{aligned} s_{1,(i,j)} &= \frac{c_{-1,-1}}{L_i} \left(\mathbf{v_{-1}} \otimes \mathbf{v_{-1}}\right)^{\mathbf{t}} \mathbf{u_{i,j}}\,, \\ s_{2,(i,j)} &= \frac{c_{-1,0}}{L_i} \left(\mathbf{v_{-1}} \otimes \mathbf{v_{-1}}\right)^{\mathbf{t}} \mathbf{u_{i,j}} + \frac{c_{-1,1}}{L_i} \left(\mathbf{v_{-1}} \otimes \mathbf{v_1}\right)^{\mathbf{t}} \mathbf{u_{i,j}}\,, \\ s_{3,(i,j)} &= c_{1,-1} L_i \left(\mathbf{v_1} \otimes \mathbf{v_{-1}}\right)^{\mathbf{t}} \mathbf{u_{i,j}}\,, \\ s_{4,(i,j)} &= c_{1,0} L_i \left(\mathbf{v_1} \otimes \mathbf{v_{-1}}\right)^{\mathbf{t}} \mathbf{u_{i,j}} + c_{1,1} L_i \left(\mathbf{v_1} \otimes \mathbf{v_1}\right)^{\mathbf{t}} \mathbf{u_{i,j}}\,. \end{aligned} \quad (5.24)$$

Substituting L_i in (5.24) and following the same procedure as the corner, we can get the evolution equations for the state variables as

$$s^{n+1}_{1,(i,j)} = \frac{\hat{r}_i}{r_i} s^n_{1,(i,j)} + \frac{c_{-1,-1}}{r_i} \left(\mathbf{v_{-1}} \otimes \mathbf{v_{-1}}\right)^{\mathbf{t}} \left(\mathbf{u_{i,j}}^{n+1} - \mathbf{u_{i,j}}^{n}\right), \quad (5.25)$$

$$\begin{aligned} s^{n+1}_{2,(i,j)} = \frac{\hat{r}_i}{r_i} s^n_{2,(i,j)} &+ \frac{c_{-1,0}}{r_i} \left(\mathbf{v_{-1}} \otimes \mathbf{v_{-1}}\right)^{\mathbf{t}} \left(\mathbf{u_{i,j}}^{n+1} - \mathbf{u_{i,j}}^{n}\right) + \\ &\frac{c_{-1,1}}{r_i} \left(\mathbf{v_{-1}} \otimes \mathbf{v_1}\right)^{\mathbf{t}} \left(\mathbf{u_{i,j}}^{n+1} - \mathbf{u_{i,j}}^{n}\right), \end{aligned} \quad (5.26)$$

$$s_{3,(i,j)}^{n+1} = s_{3,(i,j)}^{n} + c_{1,-1}\left(\mathbf{v_1}\otimes\mathbf{v_{-1}}\right)^{\mathbf{t}}\left(r_i{\mathbf{u_{i,j}}}^{n+1} - \hat{r}_i\mathbf{u_{i,j}}^{n}\right), \tag{5.27}$$

$$\begin{aligned} s_{4,(i,j)}^{n+1} = s_{4,(i,j)}^{n} &+ c_{1,0}\left(\mathbf{v_1}\otimes\mathbf{v_{-1}}\right)^{\mathbf{t}}\left(r_i{\mathbf{u_{i,j}}}^{n+1} - \hat{r}_i\mathbf{u_{i,j}}^{n}\right) + \\ &+ c_{1,1}\left(\mathbf{v_1}\otimes\mathbf{v_1}\right)^{\mathbf{t}}\left(r_i{\mathbf{u_{i,j}}}^{n+1} - \hat{r}_i\mathbf{u_{i,j}}^{n}\right). \end{aligned} \tag{5.28}$$

The stiffness matrices and the state variable force are given by

$$\mathbf{K_{L,e_x}} = \underset{\substack{i=1,..,m_x \\ j=-\infty,..,-1}}{\mathbb{A}} \left\{ \begin{array}{l} \frac{c_{-1,-1}}{r_i}\mathbf{A_{-1}}\otimes\mathbf{A_{-1}} + \frac{c_{-1,0}}{r_i}\mathbf{A_{-1}}\otimes\mathbf{A_0} + \frac{c_{-1,1}}{r_i}\mathbf{A_{-1}}\otimes\mathbf{A_1} + \\ + c_{0,-1}\mathbf{A_0}\otimes\mathbf{A_{-1}} + c_{0,0}\mathbf{A_0}\otimes\mathbf{A_0} + c_{0,1}\mathbf{A_0}\otimes\mathbf{A_1} + \\ + c_{1,-1}r_i\mathbf{A_1}\otimes\mathbf{A_{-1}} + c_{1,0}r_i\mathbf{A_1}\otimes\mathbf{A_0} + c_{1,1}r_i\mathbf{A_1}\otimes\mathbf{A_1} \end{array} \right\}, \tag{5.29}$$

$$\mathbf{K_{R,e_x}} = \underset{\substack{i=1,..,m_x \\ j=-\infty,..,-1}}{\mathbb{A}} \left\{ \begin{array}{l} \frac{c_{-1,-1}}{r_i}\mathbf{A_{-1}}\otimes\mathbf{A_{-1}} + \frac{c_{-1,0}}{r_i}\mathbf{A_{-1}}\otimes\mathbf{A_0} + \frac{c_{-1,1}}{r_i}\mathbf{A_{-1}}\otimes\mathbf{A_1} + \\ + c_{0,-1}\mathbf{A_0}\otimes\mathbf{A_{-1}} + c_{0,0}\mathbf{A_0}\otimes\mathbf{A_0} + c_{0,1}\mathbf{A_0}\otimes\mathbf{A_1} + \\ + c_{1,-1}\hat{r}_i\mathbf{A_1}\otimes\mathbf{A_{-1}} + c_{1,0}\hat{r}_i\mathbf{A_1}\otimes\mathbf{A_0} + c_{1,1}\hat{r}_i\mathbf{A_1}\otimes\mathbf{A_1} \end{array} \right\}, \tag{5.30}$$

$$\mathbf{F_{sv,e_x}^n} = \underset{\substack{i=1,..,m_x \\ j=-\infty,..,-1}}{\mathbb{A}} \left\{ \begin{array}{l} \mathbf{v_{-1}}\otimes\mathbf{v_{-1}}\frac{\hat{r}_i}{r_i}s_{1,(i,j)}^{n} + \mathbf{v_{-1}}\otimes\mathbf{v_1}\frac{\hat{r}_i}{r_i}s_{2,(i,j)}^{n} + \\ + \mathbf{v_1}\otimes\mathbf{v_{-1}}s_{3,(i,j)}^{n} + \mathbf{v_1}\otimes\mathbf{v_1}s_{4,(i,j)}^{n}. \end{array} \right\}. \tag{5.31}$$

A similar procedure can be followed to get the contributions from the edge exterior along y. Thus, the combined system of equations for the exterior can be written as

$$\mathbf{K_L U_e^{n+1}} = {\mathbf{F_e}}^{n+1} + \mathbf{F_{sv}^n} + \mathbf{K_R U_e^n} \tag{5.32}$$

where

$$\mathbf{K_L} = \mathbb{A}\left\{\mathbf{K_{L,c_{xy}}}, \mathbf{K_{L,e_y}}, \mathbf{K_{L,e_x}}\right\} + \bar{\mathbf{P}} \tag{5.33}$$

$$\mathbf{K_R} = \mathbb{A}\left\{\mathbf{K_{R,c_{xy}}}, \mathbf{K_{R,e_y}}, \mathbf{K_{R,e_x}}\right\} \tag{5.34}$$

$$\mathbf{F_{sv}^n} = \mathbb{A}\left\{\mathbf{F_{sv,c_{xy}}^n}, \mathbf{F_{sv,e_x}^n}, \mathbf{F_{sv,e_y}^n}\right\} \tag{5.35}$$

5.3 Numerical Experiment: 2D Discrete Wave Equation

The wave equation for a discrete half-space in 2D ($x \geq 0 \cup y \geq 0$) given by:

$$-D_x^2 u - D_y^2 u + \frac{\partial^2 u}{\partial t^2} = f. \tag{5.36}$$

The domain of interest has 100 atoms along each dimension and the external force is applied at the node at position $(75, 75)$ of the square lattice. The domain of interest here is taken

larger than the 1D problem so that the wave reflections can be seen clearly at the edges. The simulation is performed using both MD-PMDL and continuous PMDL boundary conditions and compared with the exact solution that is obtained by simulating a much larger domain. The parameters for both PMDL and MD-PMDL are taken as $\{(p_i, q_i) = (0, 1)\}$. The loading and initial conditions are given by

$$f(75, 75, t) = \begin{cases} 10 * sin(0.9 * \pi t)^2 & t < 100\left(\frac{\pi}{0.9}\right) \\ 0 & \text{otherwise} \end{cases} \tag{5.37}$$

$$u(i, j, 0) = 0 \tag{5.38}$$

$$\dot{u}(i, j, 0) = 0 \tag{5.39}$$

Fig.(5.3) shows the energy contours at $t = 100$. The figure clearly shows significant reflection at the corner boundary for continuous PMDL as compared to hardly any reflections for MD-PMDL boundary conditions. Also, Fig.(5.3) shows the error evolution over the duration of the simulation and again the superior absorption properties of MD-PMDL are clearly seen(MD-PMDL has an error of $< 1\%$ while Continuous PMDL's error reaches 9%). Based on the 1D and 2D results, we can conclude that MD-PMDL is more accurate in phonon absorption than continuous PMDL.

5.4 Numerical Experiment: Mode 3 Fracture

In this simulation, a semi-infinite strip with an initial crack is subjected to out-of-plane displacements resulting in a steady growth of the initial crack. The aim of the simulation is to see the effectiveness of MD-PMDL in absorbing the phonons emitted due to the breaking of bonds during crack propagation. While this is not a full fledged crack propagation simulation, it gives an idea of the usefulness of MD-PMDL in a realistic fracture simulation involving moving boundaries(which is out of scope of this thesis). This example also illustrates the applicability of MD-PMDL where the interior is nonlinear.

We use the Slepyan model of fracture in which the atoms are connected to the neighbors through bonds that are elastic when the deformation is less than a limit,$u_f = 2$, and snap when the deformation exceeds the limit. We use the same setup as in [15] to study the effect of the high frequency phonons that are emitted when the bonds break. The setup

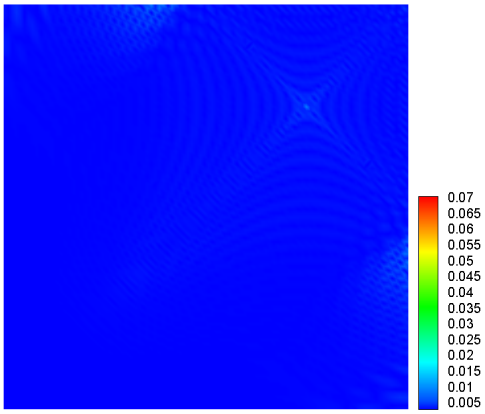

(a) MD-PMDL is used as the boundary condition. There is almost no reflection near the boundary.

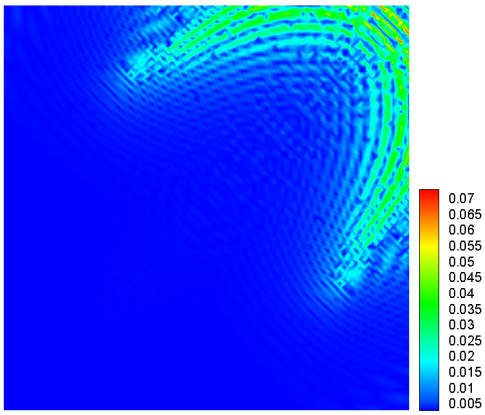

(b) Continuous PMDL is used as the boundary condition. Significant reflections can be seen in the region near the boundaries.

Figure 5.2: The energy contours at $t = 100$ for the 2D discrete wave equation using (a)MD-PMDL and (b)continuous PMDL boundary conditions.

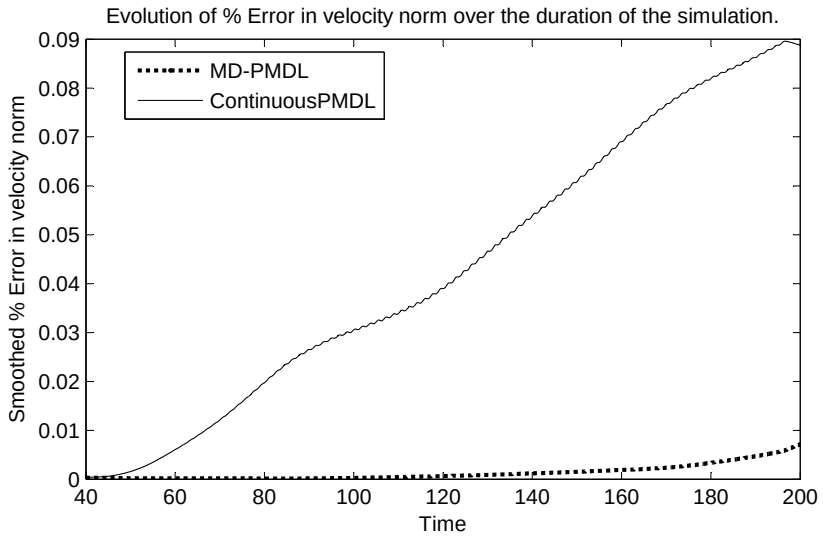

Figure 5.3: Plot of the evolution of Error in velocity norm over the simulation duration.

is as shown in Fig(5.4(a)). The interior is a rectangular grid that is 20 atoms wide and 100 atoms long. The initial crack is taken to be 20 atoms long.

The exterior region is approximated using MD-PMDL using 5 identical layers with parameters $\{(p_i, q_i) = (0, 1)\}$. The other boundary condition used for comparison, is essentially a buffer region that is 10 atoms wide with a dirichlet condition at the end. Also, dirichlet conditions $u = +U, -U$, is applied at the top and bottom row of atoms. The dirichlet condition at the left edge is taken to be $+U$ for atoms above the crack and $-U$ for the atoms below the crack, and for the right edge is taken to vary linearly from $-U$ at the bottom row to $+U$ at the top row. Also, for the atoms outside the initial cracked zone, the initial displacements are taken to vary linearly between the dirichlet conditions at the top and bottom rows. For the atoms in the cracked zone, the initial conditions are taken to vary linearly between the dirichlet condition at the left edge and the initial displacement immediately to the right of the crack tip. The value of U is taken to be 20 for this simulation. The initial velocities are taken to be zero over the entire domain.

In [15], the author uses moving boundaries to simulate a steady state crack growth. However, steady state is not simulated in this example, and the crack is allowed to grow from initial configuration until it reaches the end of the domain. A velocity norm is measured for small region (40 atoms wide) near the left boundary to see the effect of reflections due

to phonon. The simulations are carried out for MD-PMDL and a truncated boundary with an offset of 10 atoms. The results are compared against the exact solution obtained using a much larger domain. Fig(5.4(b)) shows the error in velocity norm and it is clear that MD-PMDL performs better than a truncated boundary(MD-PMDL has $< 5\%$ error while truncated BC has almost 30% error). Though the magnitude of the values are small, this would be significant in an actual fracture simulation with moving boundaries as the domain size would be small and reflection of phonon back into the domain will be a major problem. This also demonstrates that MD-PMDL performs well for the case of non-linear interaction in the interior domain.

(a) A schematic of the setup for crack simulation.

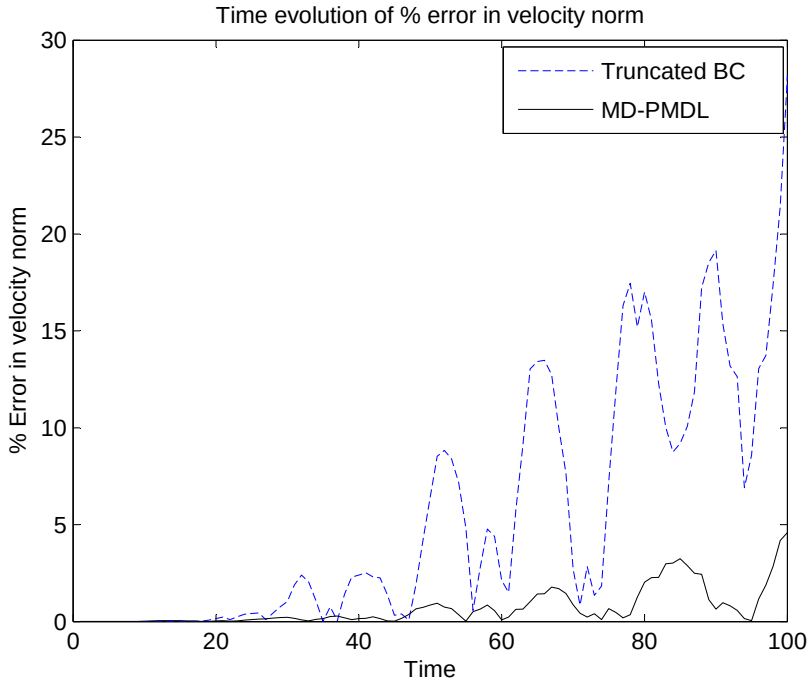

(b) Plot of the relative Error in velocity norm at a small region(40 atoms wide) near the left boundary.

Figure 5.4: Simulation of Mode 3 crack propagation.

Chapter 6

Concluding Remarks

We have presented a systematic procedure to develop ABC's for MD domains and have demonstrated through numerical examples that they are superior in performance compared to their continuum counterpart. This validates our initial assertion that a continuous ABC cannot be used directly for the MD domain.

We also presented an explicit expression for the error estimate in terms of the parameters of the boundary condition. The error estimate makes the approximation characteristics of the boundary condition transparent, indicating that it can be easily optimized for performance.

The final form of the boundary conditions for 1D and 2D lattices is presented in an explicit form that is easy to implement. We note that while the boundary condition couples the domain along the boundary, it is still local to the region near the boundary. Since the error decays exponentially with the number of layers, often only a few layers are needed to obtain accurate results. Thus, the additional overhead due to MD-PMDL is not high. Also the method does not involve any expensive convolution operations as it is *completely* local in time. The only computational burden is the solution of sparse linear system (factorization needs to be done just once). While explicit comparison with other existing MD-ABC's is not made, we believe that the local nature of MD-PMDL provides an efficient alternative to existing MD-ABC's.

While MD-PMDL's effectiveness was illustrated for a square lattice with scalar field variable, the derivation of MD-PMDL is applicable for a vector equation. Thus, it should be possible to extend MD-PMDL for more complex lattices by expressing them as a

simple lattice with multiple degrees of freedom per node. However, complex lattices involve optical phonon branches that are similar to dispersion branches for elastic wave propagation in continuous waveguides. Since PMDL has stability issues in simulating elastic waves in layers [13], we anticipate that the extension to complex lattices might not be straightforward and would be investigated in the future.

The current formulation is limited to the case of zero temperature in the exterior. For a more realistic simulation, MD-PMDL should be extended to handle non-zero temperatures in the exterior. This extension to non-zero temperature would be investigated in the near future.

Another area of focus is the extension of MD-PMDL as an interface condition for atomistic-continuum coupling. While interface conditions act like an ABC in dissipating the high frequency phonons, they also need to enable the exchange information with the continuum domain. A related extension would be for moving boundaries as seen in the numerical experiment involving crack propagation.

A minor disadvantage of MD-PMDL is that the atoms are coupled along the boundary. However such coupling is limited to the neighboring super-atoms. Furthermore, the MD-PMDL equations are completely linear. The linearity and local coupling will be utilized to develop effective linear solution techniques that would require minimal computational cost.

Bibliography

[1] D. Givoli. Non-reflecting boundary conditions : A review. *Journal of Computational Physics*, 94:1–29, 1991.

[2] W. Cai, M. D. Konin, V. V. Bulatov, and S. Yip. Minimizing boundary reflections in coupled-domain simulations. *Physical Review Letters*, 85:3213–3216, 2000.

[3] E. G. Karpov, G. J. Wagner, and W. K. Liu. A green's function approach to deriving non-reflecting boundary conditions in molecular dynamics simulations. *Int. J. Numer. Methods Engrg.*, 62(9):1250–1262, 2005.

[4] G. J. Wagner, E. G. Karpov, and W. K. Liu. Molecular dynamics boundary conditions for regular crystal lattices. *Comput. Method Appl. Mech. Engrg.*, 193:1579–1601, 2004.

[5] J. P. Berenger. A perfectly matched layer for the absorption of electromagnetic waves. *Journal of Computational Physics*, 114:185–200, 1994.

[6] W. C. Chew and W. H. Weedon. A 3-d perfectly matched medium from modified maxwells equations with stretched coordinates. *Microwave and Optical Technology Letters*, 7:599–604, 1994.

[7] T. Hagstrom. *New results on absorbing layers and radiation boundary conditions.*, pages 1–42. Topics in Computational Wave Propagation. Springer, New York, 2003.

[8] A. C. To and S. Li. Perfectly matched multiscale simulations. *Phys. Rev. B*, 74:035414, 2005.

[9] A. C. To and S. Li. Perfectly matched multiscale simulations for discrete systems: Extension to multiple dimensions. *Phys. Rev. B*, 74:045418, 2006.

[10] X. Li and W. E. Variational boundary conditions for molecular dynamics simulations of solids at low temperature. *Communications in Computational Physics*, 1:136–176, 2006.

[11] W. E and Z. Huang. Matching conditions in atomistic-continuum modeling of material. *Physical Review Letters*, 87:135501, 2001.

[12] M. N. Guddati and K. W. Lim. Continued fraction absorbing boundary conditions for convex polygonal domains. *International Journal for Numerical Methods in Engineering*, 66:949–977, 2006.

[13] M.N. Guddati, K.W. Lim, and M.A. Zahid. Perfectly matched discrete layers for unbounded domain modeling. In Ed. F. Mogoules, editor, *Computational Methods for Acoustics*, pages 1–42. Saxe-Coburg, London, 2007.

[14] M. N. Guddati. Arbitrarily wide-angle wave equations for complex media. *Comput. Methods Appl. Mech. Engrg.*, 195:65–93, 2006.

[15] M. Marder and S. Gross. Origin of crack tip instabilities. *J. Mech. Phys. Solids*, 43:1–48, 1995.